Lappeenranta-Lahti University of Technology LUT
School of Engineering Science
Technical Physics
Master's Programme in Computational Engineering and Technical Physics

Irina Sheina

DETERMINATION OF THE CHEMICAL COMPOSITION OF MATERIALS BY RAMAN SPECTROSCOPY

Examiners: Professor Erkki Lähderanta
Researcher Egor Fadeev

Supervisors: Professor Erkki Lähderanta
Researcher Egor Fadeev

ABSTRACT

Lappeenranta-Lahti University of Technology LUT
School of Engineering Science
Technical Physics
Master's Programme in Computational Engineering and Technical Physics

Irina Sheina

Determination of the chemical composition of materials by Raman spectroscopy

Master's Thesis

60 pages, 47 figures, 1 table

Examiners: Professor Erkki Lähderanta
Researcher Egor Fadeev

Keywords: Raman spectroscopy, Raman spectral imaging, dispersive spectrometer

This work is devoted to the phenomenon of Raman scattering of light. The fundamental principles underlying this phenomenon are studied and described, factors that influence the registered signal are identified, and the main techniques based on the Raman method are considered. Two basic types of Raman spectrometers, dispersive and Fourier transform are compared. Much attention is paid to the structure of the spectrometer and the principle of its operation. The experimental part was performed using the Horiba Jobin-Yvon LabRam HR800 spectrometer. To verify the correct operation of the spectrometer, the Raman spectra of mica, paraffin, polyethylene, and polypropylene were obtained and compared with reference ones. The main practical task of this work was to search for microplastic particles on the surface of a contaminated filter using the Raman spectral mapping function. The results showed the absence of the desired substances in the limited analyzed area of the filter, but some other chemical elements were identified. The problems associated with the mapping duration of the entire surface and the complexity of the subsequent processing of results make further analysis difficult.

ACKNOWLEDGMENTS

This thesis would not happen to be possible without the guidance of my supervisors. I would first like to thank Professor Erkki Lahderanta for his help in choosing a topic and support throughout the process of researching and writing this thesis. I would also like to express my deep and sincere gratitude to him for the great opportunity to study at the Lappeenranta University of Technology. Special thanks to research assistant Egor Fadeev. I very much appreciate his valuable comments on this thesis and advice throughout the work.

I would like to express my very profound gratitude to my parents - Yuri and Valentina, for their endless love, unfailing support, and continuous encouragement over all my years of study.

Above all, thank you, Lord, for always being there for me.

Lappeenranta, May 2020

Irina Sheina

TABLE OF CONTENTS

LIST OF ABBREVIATIONS

1D	One-dimensional
2D	Two-dimensional
3D	Three-dimensional
CARS	Coherent anti-Stokes Raman spectroscopy
CCD	Charge-coupled device
IR	Infrared
FWHM	Full width at half-maximum
He-Ne	Helium-neon
LED	Light-emitting diode
MOS	Metal Oxide Semiconductor
RRS	Resonant Raman spectroscopy
RSOT	Optical trapping-Raman spectroscopy
SERS	Surface-enhanced Raman spectroscopy
TERS	Tip-enhanced Raman spectroscopy

INTRODUCTION

Spectroscopy applications for qualitative and quantitative analysis of substances have become widespread at present, both in terms of the number of analyses performed and the variety of analytical objects. Spectroscopic methods of analysis are very diverse, but they are all based on the interaction of the atoms, molecules, or ions that make up the analyte with electromagnetic radiation. This interaction is manifested in the absorption or emission of photons. Depending on which particles form the analytical signal, there are atomic spectroscopy methods and molecular spectroscopy methods [1].

In atomic spectroscopy, we are talking about qualitative and quantitative determination of chemical elements in different substances and concentration ranges. This includes, for example, methods of atomic absorption, atomic emission, and X-ray fluorescence.

Molecular spectroscopy methods are used to search for information about the bonds and structure of molecules. The main methods of molecular spectroscopy are based on the processes of interaction of infrared radiation with matter (Infrared spectroscopy) and Raman scattering of light (Raman spectroscopy). They are widely used to provide information about chemical structure and physical form, to identify substances by characteristic spectral patterns, and to quantify a substance in a sample. Samples can be examined in different physical states: in solids, liquids, or vapors, in hot or cold states, in bulk, microscopic particles, or surface layers. The methods are very diverse and provide solutions to many interesting and complex analytical problems [2].

Raman spectroscopy has several advantages compared with other methods of vibrational spectroscopy, for example, such as IR Fourier and near-IR spectroscopy. The advantages are a consequence of the fact that the Raman Effect is observed in the scattered light from the sample and not in the light absorption spectrum by the sample. Therefore, Raman spectroscopy does not require special sample preparation and it is insensitive to absorption bands. This property of Raman spectroscopy facilitates direct measurement in solid, liquid, and gaseous media, as well as measurements through transparent materials, such as glass, quartz, and plastic [3].

The topic of this work is the study of the Raman spectroscopy method, the investigation of the main processes and laws underlying it, the understanding of the structure and principle of operation of the Horiba Jobin-Yvon LabRam HR800 Raman spectrometer, and the direct solution of practical problems related to the determination of the materials spectra.

RAMAN THEORY

1.1. Theoretical background and principles of Raman scattering

Raman spectroscopy is based on the process of inelastic photon scattering, which involves energy transfer between the incident light and matter molecules. As a result, the emitted photons change the initial wavelength in a greater or lesser direction.

When the energy of the incident photon is not large enough to excite the molecule from the ground state to the lowest electronic state, the molecule will be excited to the so-called virtual state. An electron in an excited molecule cannot remain in a virtual state for long, and therefore it immediately returns to a state with lower energy. If the electron returns to its original state (in this case, the ground state), the wavelength of the emitted photon will be the same as that of the incident photon of light. This scattering phenomenon is known as Rayleigh scattering (Fig. 1) [4].

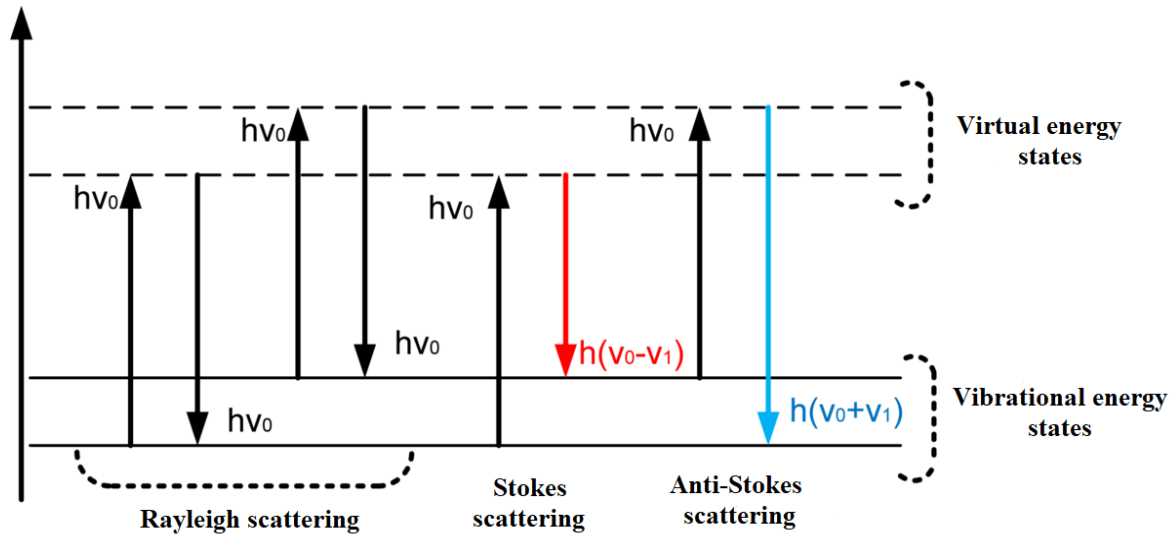

Fig.1. Diagram showing the changes in the energy state during Rayleigh and Raman scattering [5].

On the other hand, the electron can also go down to a state different from the one from which it was excited. This leads to a difference in energy between the incident photon and the emitted photon, and therefore to a shift in the wavelength of the emitted photon compared to the incident photon. This is known as Raman scattering. In this case, two possible options can be observed, namely, Stokes and anti-Stokes scattering (Fig. 1) [6].

Stokes shift is observed if the photon energy is transmitted to the molecule, resulting in scattered light with a longer wavelength and lower energy. In the molecule, the ground-state electron is excited from an original lower vibrational sublevel to a higher sublevel. Anti-Stokes

shift occurs when energy is transferred from the molecule to the photon. In this case, light with a shorter wavelength and higher energy is observed. The ground state electron in the molecule moves from an original higher vibrational energy sublevel to a lower sublevel. Molecular bonds vibrate at a lower frequency. In Stokes and anti-Stokes scattering, only one quantum of energy is exchanged. The absolute energy difference between incident and scattered radiation is the same for Stokes and anti-Stokes Raman scattering (indicated as $h\upsilon_1$ in Fig. 1) [7].

Energy transfer actually occurs as a two-photon process: a photon interacts with the electron cloud of the molecule, causing a dipole moment and changing the energy levels of electron vibrations; and this causes the emission of a second photon in response to these changes. However, since this occurs through a single quantum mechanical process, it should not be considered as separate stages of absorption and radiation.

It should be noted that the Raman effect is relatively weak. Only approximately one photon in a hundred million (0.000001 %) will have frequency offset from the original laser radiation frequency [8].

A monochromatic light source, a laser, is used to generate and subsequently to detect a sufficient number of scattered photons. The Raman spectrometer counts the number of displaced photons as a function of their wavelengths to generate the spectrum. The full Raman spectrum is symmetrical with respect to the incident light wavelength, however, the Stokes and anti-Stokes parts will not mirror each other due to their relative difference in intensity [4].

In thermal equilibrium, the population of vibrational levels obeys the Boltzmann distribution, that is, the population of higher energy levels decreases exponentially. Accordingly, the exited level is much less populated than the zero level, which leads to a much lower intensity of anti-Stokes lines in the Raman spectrum compared to the intensity of Stokes lines.

1.2. Raman spectrum

As a rule, the Raman spectrum refers to the Stokes part, which is more intense. The reference frequency is the frequency of Rayleigh scattering (i.e., the frequency of the radiation source), and the frequency of the line in the spectrum is calculated by subtracting the frequency of the Stokes line from the frequency of Rayleigh radiation (Fig. 2) [9].

The X-axis units for Raman spectra are wavenumbers (cm^{-1}), which allows us to compare the Raman spectra regardless of the incident light wavelength. Strictly speaking, Raman scattering should be expressed as an energy shift compared to the incident radiation energy and should be denoted as $\Delta\ cm^{-1}$, but often it is expressed as cm^{-1} for simplicity [10].

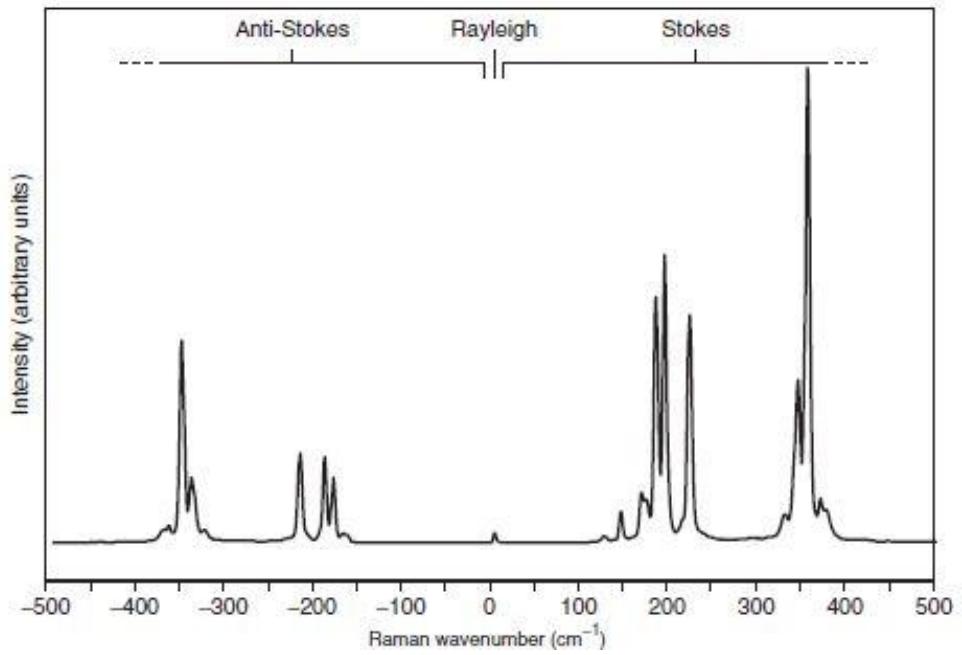

Fig. 2. The full Raman spectrum of pararealgar As_4S_4. The actual intensity of the Rayleigh line is suppressed by a notch filter in the spectrometer [9].

Raman spectra are very sensitive to the nature of chemical bonds - both in organic molecules and polymer materials, and in inorganic crystal lattices and clusters [10]. For this reason, each substance has its own individual Raman spectrum, which is analogous to the "fingerprint" (Fig.3).

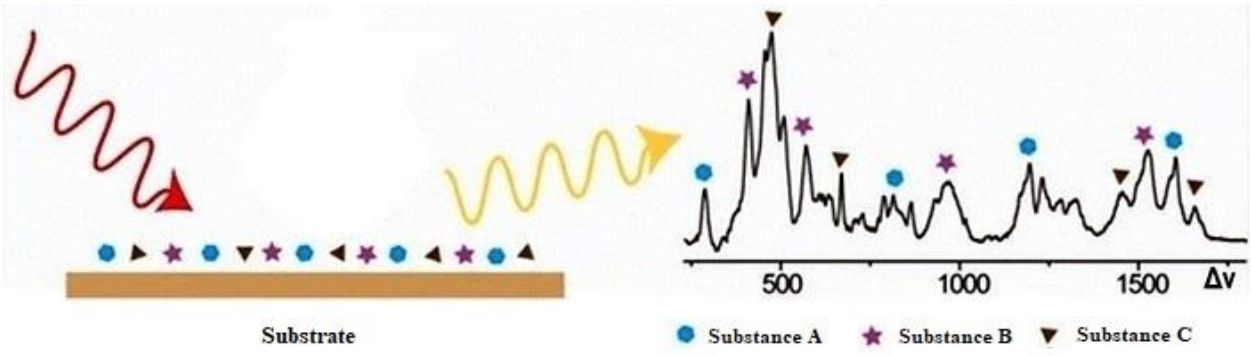

Fig. 3. Identification of various elements by key peaks on the Raman spectrum of a complex mixture [11].

The spectra of organic materials mainly consist of lines that correspond to deformation and valence vibrations of chemical bonds of carbon (C) with other elements, usually hydrogen (H), oxygen (O) and nitrogen (N), as well as characteristic vibrations of various functional groups

(hydroxyl $-OH$, amino $-NH_2$, etc.). These lines appear in the range from 600 cm^{-1} (valence vibrations of single $C-C$ bonds) to 3600 cm^{-1} (vibrations of the hydroxyl $-OH$ group). It is important to note that the position of the maxima of the peaks in the Raman spectrum, characterizing the fluctuations of single $C—C$, double $C=C$, and triple $C\equiv C$ bonds, differs. In addition, deformational vibrations of aliphatic chains are manifested in the spectra of some organic compounds in the range of 250 - 400 cm^{-1} [12].

The spectra of crystal lattices contain lines corresponding to the scattering of radiation on the collective excited states of the lattice: optical and acoustic phonons, plasmons, and magnons [13]. The Raman spectra of diatomic gases consist of lines corresponding to the rotational and vibrational-rotational transitions of molecules.

1.2.1. Parameters of the Raman spectrum

The main parameters of the Raman lines used for analysis are:

a) wavenumber ν, equal to the frequency of one of the oscillatory processes in the material. It determines the position of the line with respect to the exciting line (Rayleigh scattering line) (Fig. 4).

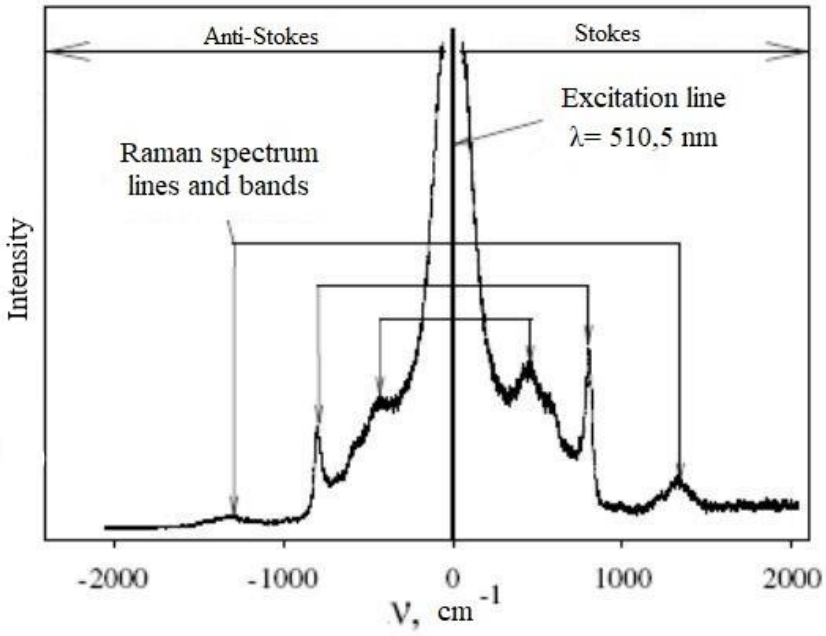

Fig. 4. The total Raman spectrum of boron oxide B_2O_3 at a temperature of 1400 K and exciting radiation with a wavelength of λ = 510.5 nm [14].

b) the line intensity I, which characterizes the efficiency of the Raman scattering in the oscillatory process. There is a peak intensity I_0 (the distance from the top of the line to the background level), and an integral intensity I_{int} (the area bounded by the contour of the line). The latter is usually expressed in units relative to the value of a reference sample. Usually, the diamond is used as the standard. Sometimes I_{int} is expressed as a percentage of the exciting line [15];

c) FWHM (full width at half-maximum) δ of the line, equal to the distance between the points of the line contour at the height $\frac{I_0}{2}$ (Fig. 5);

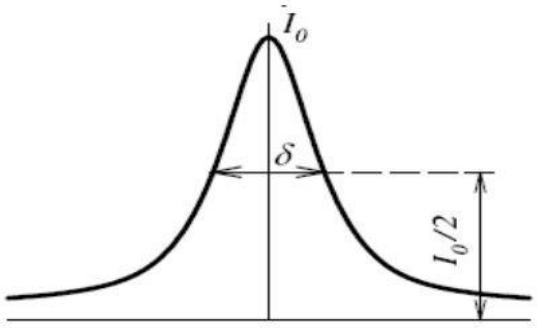

Fig. 5. The intensity and FWHM of the Raman line.

d) a depolarization ρ of the Raman line, defined as the ratio of the intensities of parallel (I_z) and perpendicular (I_x) polarized components of the Stokes line. The line is called polarized if ρ<0.75 and depolarized if ρ=0.75. Polarized lines usually correspond to completely symmetrical oscillations, while depolarized lines correspond to antisymmetric and degenerate, or generally forbidden oscillations.

Analysis of Raman spectrum is based on the values of all the above parameters.

1.2.2. Influence of fluorescence on the Raman spectrum

One of the most significant problems of the Raman method is fluorescence [8]. Fluorescence is strong radiation from a sample, being several times stronger than the Raman signal. Even minor fluorescence can overlap the Raman signal (Fig. 6).

Fluorescence occurs when a sample is irradiated with a relatively high-energy laser, i.e. laser of a small wavelength. Under the influence of an incident light beam, the molecule passes into an excited energy state. Further, through a non-radiative transition, the molecule relaxes to a lower electronic level. From this level, the molecule returns to its ground state, emitting a photon.

Fluorescence can be avoided by using a laser with longer wavelength, and the energy of the exciting photons will be too small to transfer the molecule to an excited energy state [9]. It would seem that since increasing the wavelength of the light source prevents fluorescence, it would be natural to always use long-wave lasers. However, as will be discussed later, this leads to a sharp drop in the intensity of scattered light.

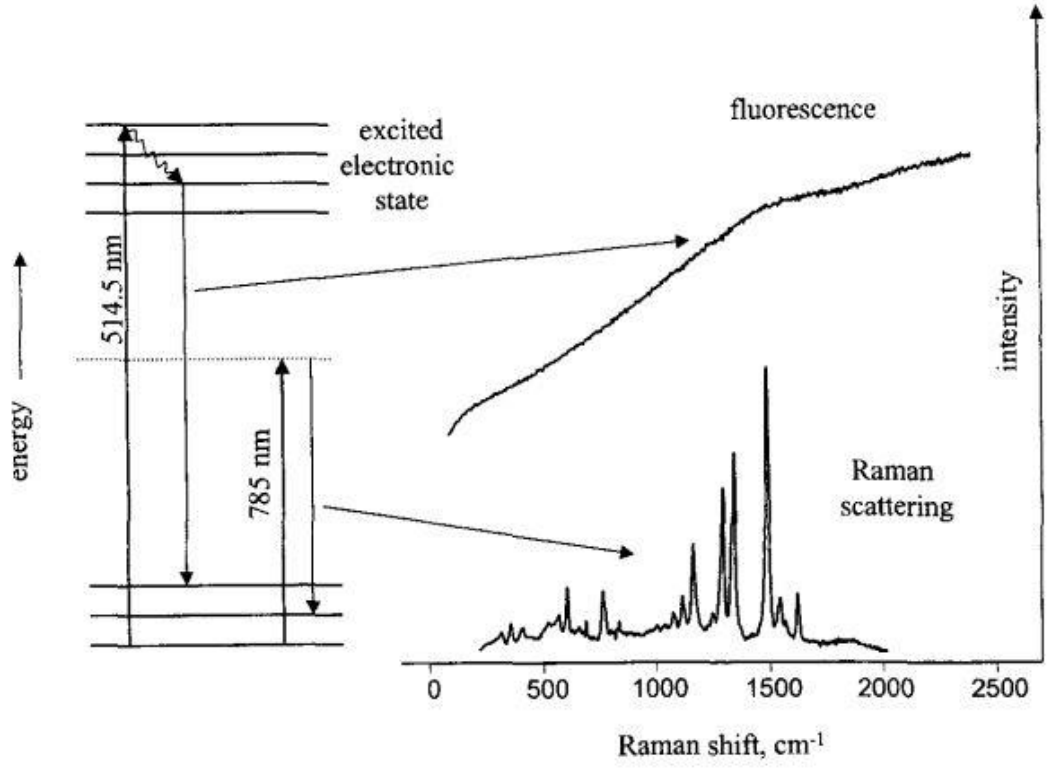

Fig. 6. Energy diagram and Raman spectra of a fluorescent sample obtained using 514.5 and 785 nm lasers. The fluorescence intensity is several orders of magnitude greater than Raman scattering [16].

The probability of fluorescence is largely determined by the nature of the test sample. When irradiated with short-wavelength lasers, many inorganic and organic molecular compounds fluoresce, which is due to their chemical structure. Organic substances are most prone to fluorescence. When they are irradiated with visible-range lasers, fluorescence is usually observed. Therefore, such lasers are used only for the analysis of inorganic compounds. For organic molecules, near-IR lasers are used.

1.2.3. Influence of the substrate material on the Raman spectrum

In some cases precise focusing of laser radiation on the sample is difficult, for instance, with small volumes of the solution, or in the case of thin layers of solid transparent substances. In such

a situation the probability of the influence of the substrate material on the Raman signal appears. To measure such samples it is necessary to select the composition of the substrate carefully to prevent extraneous peaks in the resulting spectrum. In such situations, one can use the following approaches to solve the problem.

The first option is to use as a substrate a material whose spectrum shape is primitive, for example, represents a single intense narrow peak. A vivid example, in this case, can be a substrate made of pure silicon (Fig. 7). Knowing the spectrum of the substrate material, an operator, after obtaining the spectrum of the test sample, can subtract these two spectra.

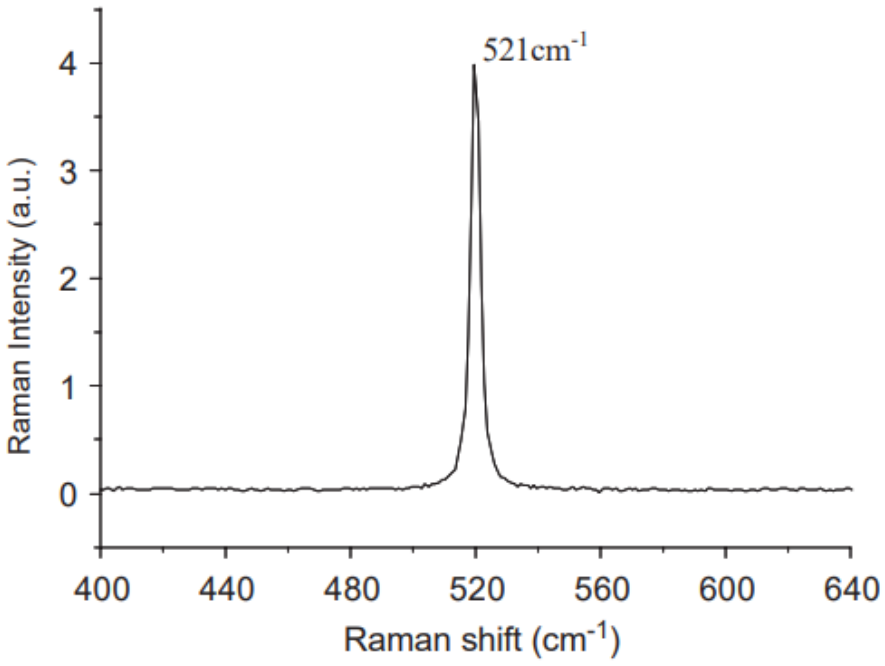

Fig. 7. A typical Raman spectrum of silicon (Si) [17].

However, this method involves the implementation of additional steps related to finding the spectrum of the substrate material and then subtracting the spectra for each measurement of the sample. In this regard, it seems more reasonable to follow a different approach.

The second option involves using a material as a substrate that contributes a minimal background signal. In [18] was made a comparison of various substrates for obtaining Raman spectra of transparent material. Sodium-calcium glass (microscope slide), quartz glass, polyethylene terephthalate, polyethylene, polytetrafluoroethylene, and aluminum foil were among the studied substances. The main criteria for choosing materials were their inertia in relation to the sample, availability, and low price.

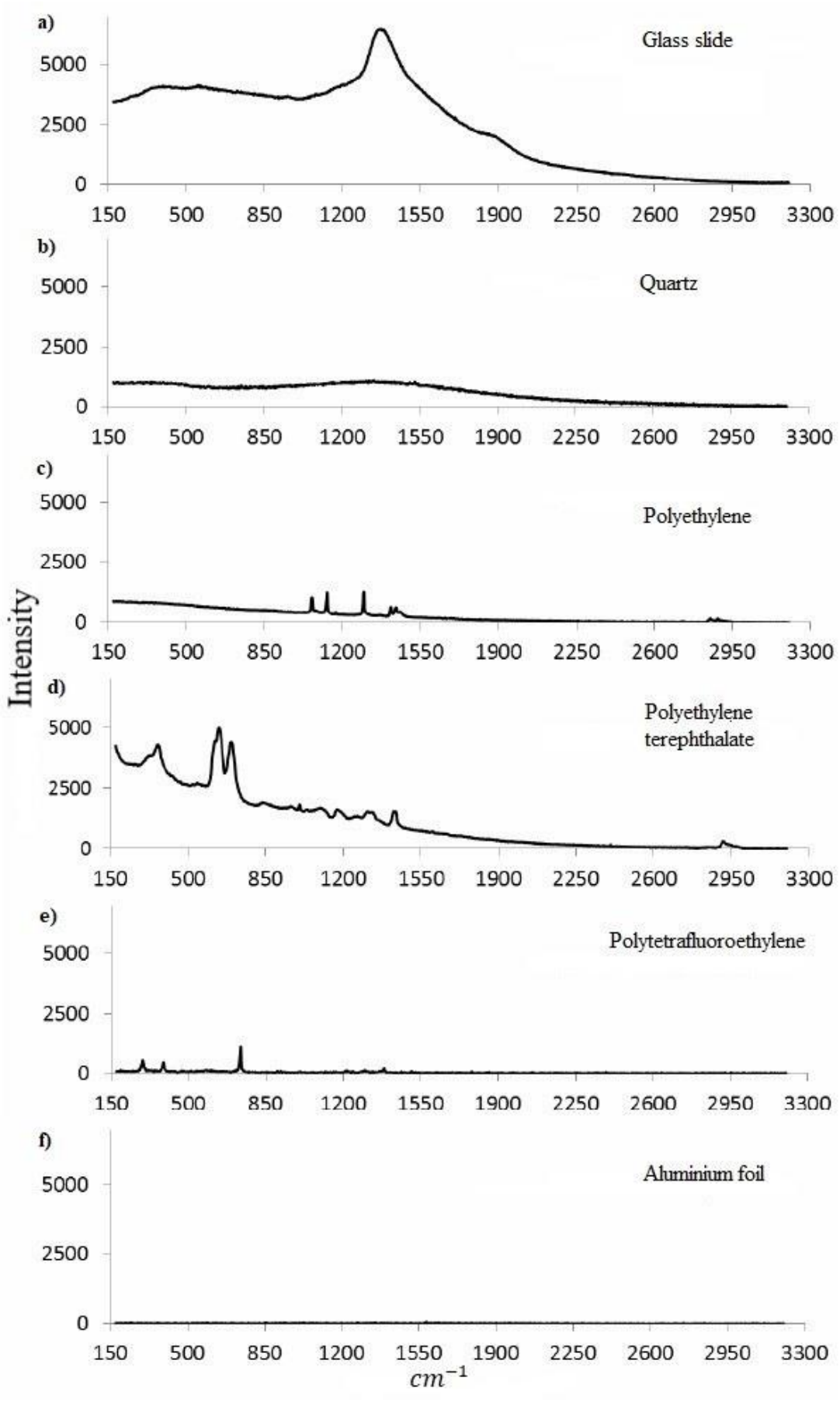

Fig. 8. Raman spectra of sodium-calcium glass (a), quartz glass (b), polyethylene (c), polyethylene terephthalate (d), polytetrafluoroethylene (e) and aluminum foil (f) [18].

A glass slide used in optical microscopy is characterized by an intense signal in almost the entire region of the obtained spectrum (Fig. 8). A less intense signal is registered when using quartz glass, however, this option is not optimal. The spectra of polymer materials such as polyethylene, polyethylene terephthalate, and polytetrafluoroethylene are characterized by narrow intense peaks corresponding to their molecular structure. The most promising substrate material for experiments was aluminum foil. It was found that the smallest background signal is observed when using aluminum foil. Possible reflection of laser radiation into the detector, in this case, is not critical since it is suppressed by the optical filters of the Raman spectrometer probe. Besides, aluminum foil is affordable and it has low cost.

1.3. Raman Techniques

Raman spectroscopy allows one to non-invasively obtain unique information about the composition and chemical bonds of molecules. However, like any method, Raman scattering has its limitations. Second significant drawback (in addition to fluorescence) is the low signal intensity. This problem is solved by various modifications of the method, such as resonant Raman spectroscopy (RRS), optical trapping-Raman spectroscopy (RSOT), coherent anti-Stokes Raman spectroscopy (CARS), tip-enhanced Raman spectroscopy (TERS) and surface-enhanced Raman spectroscopy (SERS) (Fig. 9). In total, there are now more than 25 different types of Raman spectroscopy techniques.

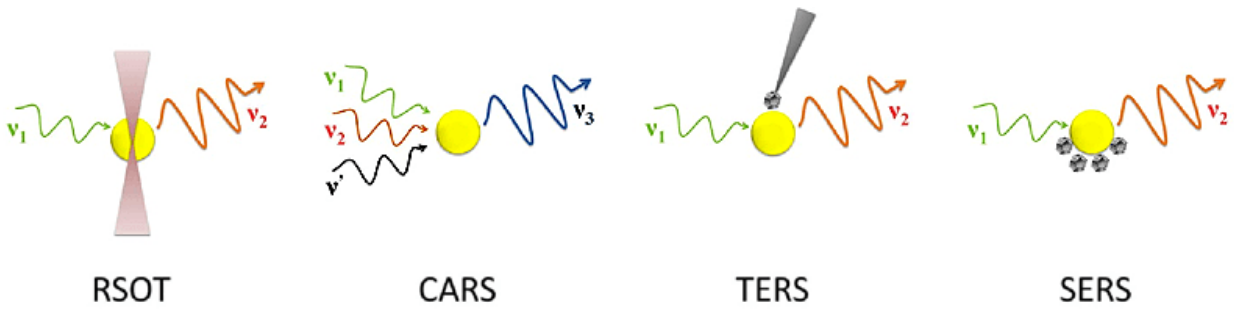

Fig. 9. Techniques to enhance the Raman signal. Designations: ν1 is the excitation frequency, ν2 is the Stokes Raman scattering, ν3 is the anti-Stokes Raman scattering, and ν′ is a variable frequency. The yellow circle indicates the molecule in question, and the gray polyhedron indicates the nanoparticle.

1.3.1. Resonant Raman spectroscopy (RRS)

The first and easiest way to increase the intensity of the Raman scattering signal is to use the resonant excitation frequency.

Resonant Raman spectroscopy is a method of Raman spectroscopy in which the energy of incident photons is close to the electron transition energy of the test material [19]. Frequency resonance leads to a significant increase in the intensity of Raman scattering, which facilitates the study of chemical compounds with low concentrations [20].

1.3.2. Optical trapping-Raman spectroscopy (RSOT)

The second method is optical trapping-Raman spectroscopy, which allows increasing the Raman intensity by increasing the signal accumulation time from single molecules [21]. This method is used to study individual particles, as well as biochemical processes in cells.

An optical tweezer is a device that allows one to manipulate microscopic objects using laser light: particles fall into the focus of the laser beam as a trap. To study cells, two laser trap beams are most often used to avoid fluctuations and rotation of the object (Fig. 10). Two beams can also be used to stretch the cell.

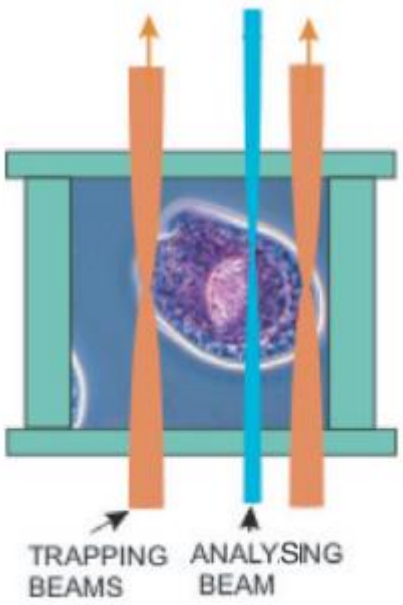

Fig. 10. Scheme of the RSAT method with two trap beams for examination single cells [21].

1.3.3. Coherent anti-Stokes Raman spectroscopy (CARS)

The method of coherent anti-Stokes Raman spectroscopy is based on the effect of resonant Raman scattering [2, 22]. This method uses three laser beams: the first source is called the pump beam ω_{pump}, the second represents the Stokes radiation with frequency ω_{Stokes}, and the third is the radiation source with a frequency ω_{probe} (Fig. 11). These beams interact with the sample and generate a coherent optical signal at the anti-Stokes frequency.

$$\omega_{CARS} = \omega_{pump} - \omega_{Stokes} + \omega_{probe} \quad (1)$$

The CARS signal ω_{CARS} resonantly increases when the difference between the pump frequency ω_{pump} and the Stokes frequency ω_{Stokes} becomes equal to the vibrational transition ω_{vib} of the molecule.

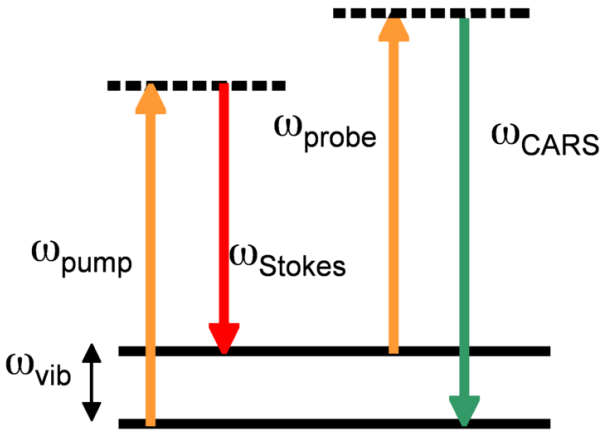

Fig. 11. CARS energy diagram [23].

In addition to higher intensity and the absence of luminescence, it is easier to distinguish near-located peaks on the CARS spectrum due to the coherence of scattered light, which is especially important, for example, when studying structurally similar substances or composite materials. Using the CARS method, great successes were achieved in the field of biology: it was possible to visualize the movement of organelles inside the cells; study the metabolism of lipids, distinguish healthy and cancerous nerve tissue by their lipid composition, etc. [24].

1.3.3. Tip-enhanced Raman spectroscopy (TERS) and surface-enhanced Raman spectroscopy (SERS)

The amplification of the Raman signal can also be achieved using noble metal nanoparticles. There are two ways to do this.

The first is to place a nanoparticle on the surface of the needle of an atomic force microscope and probe molecules, registering a Raman signal from them. In this case, the method is called tip-enhanced Raman spectroscopy (TERS) [25, 26].

In the second case, the studied molecules are placed on the surface of metal nanoparticles and the spectrum is registered in the usual way. This method is called surface-enhanced Raman spectroscopy (SERS) [11, 27]. Because of laser irradiation of metal nanoparticles with dimensions of 10-100 nm, plasmons are formed on the surface, which increases the electric field around the metal. Since the signal intensity in Raman spectroscopy is proportional to the electric field, the signal increases significantly (up to 10^{14} times) [28].

RAMAN EQUIPMENT

2.1. Raman instrumentations

The main purpose of any spectral device is the decomposition of electromagnetic radiation into monochromatic components - obtaining a spectrum. Based on this, the following main elements of the Raman spectrometer can be distinguished: a monochromatic radiation source, a device for receiving and processing a signal from the sample, and a detector (Fig. 12) [9].

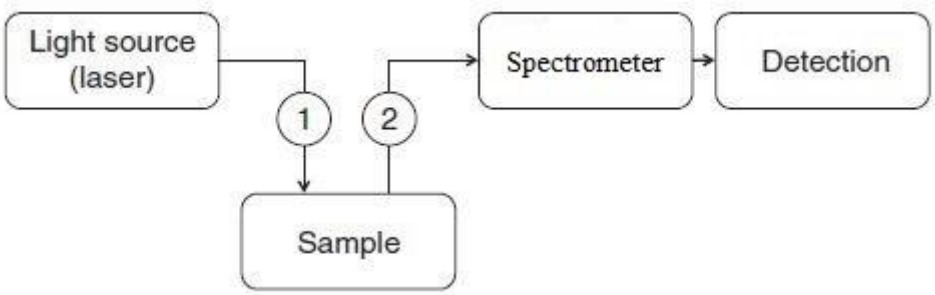

Fig. 12. Schematic diagram of the Raman spectrometer. Designations: 1 is an optical system to focus a laser beam on a sample; 2 is an optical system to collect scattered radiation.

2.1.1. Monochromatic radiation source

Since Raman spectroscopy is based on determining changes in wavelengths (frequencies), a source of monochromatic excitation is required [29]. Although the laser is the best source of excitation, not all lasers are suitable for Raman spectroscopy. The laser frequency must be extremely stable and without jumps, otherwise, this leads to errors in the Raman shift. A narrow-band laser should be used since the quality of the Raman peaks depends on the accuracy of the light source [12].

The characteristic wavelengths of the lasers used in the installation depend on the type of spectrometer, so Raman dispersive spectrometers use lasers with visible wavelengths, while typical wavelength in Fourier transform spectrometers is 1 μm.

The intensity of the scattered light, depending on various internal and external factors, is determined by the Rayleigh equation, which establishes a connection with the wavelength of the exciting light.

$$I_s \sim \frac{1}{\lambda^4} \sim \omega^4, \quad (2)$$

where I_s is the intensity of scattered light;

λ is the wavelength of the incident light;

ω is the frequency of incident light.

Thus, the Raman scattering efficiency increases significantly with a decrease in the laser radiation wavelength, which gives an advantage to short-wave lasers. However, as mentioned earlier, the widespread use of shorter wavelength lasers is hindered by the phenomenon of fluorescence. The main task of the researcher when choosing the laser wavelength is to find a compromise between these two opposing processes [22].

The ability to minimize the effect of fluorescence without narrowing the spectral range or resolution makes 785 nm lasers standard for use in this industry. However, to increase sensitivity to inorganic molecules, lasers of shorter wavelengths should be used.

2.1.1.1. The principle of laser operation

The main part of the Raman scattering experiments in this work was performed using a He-Ne gas laser with a wavelength of λ = 632.8 nm. Next we consider the key structural components and the principle of laser operation on its example.

As known, any laser consists of three main components: an active medium in which the population inversion of atomic levels is realized and photons are generated, a pumping that creates the population inversion, and an optical cavity - a device that creates positive feedback.

The active medium of a helium-neon laser is a mixture of helium and neon in a 5:1 ratio, located in a glass envelope under low pressure, usually about 300 Pa. Pumping is carried out by means of an electric discharge between the electrodes (anode and cathode) located at the ends of the tube; they are supplied with a voltage of about 1000-5000 V, depending on the length of the tube. The resonator of such a laser usually consists of two mirrors, one completely reflecting and the other transmitting about 1% of the incident radiation (Fig. 13); the typical resonator size is from 15 cm to 2 m, the output power varies from 1 to 100 mW [15].

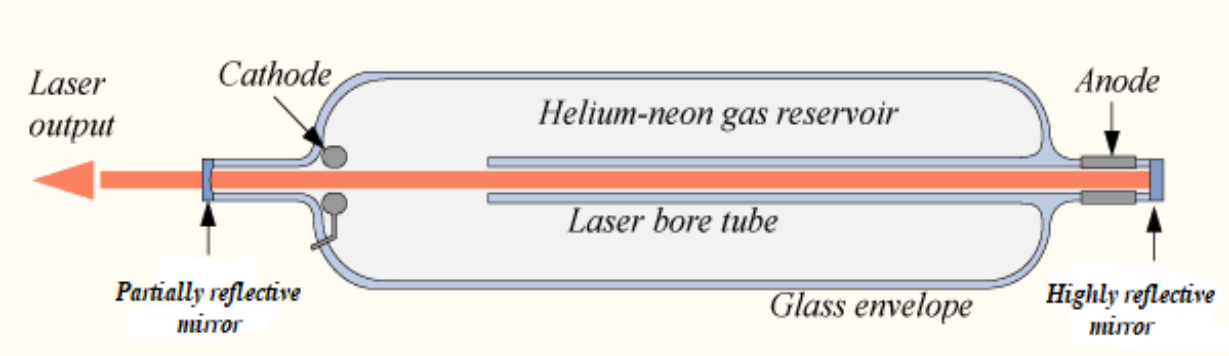

Fig. 13. Schematic diagram of a He-Ne laser [30].

Electrons, which appeared because of an electric discharge between the anode and cathode, excite helium atoms in collisions, transferring them from the ground energy state to the excited state (Fig. 14). Then, upon collisions of these helium atoms with neon atoms, the latter are excited in the same way and moved to one of the metastable energy levels. As a result, population inversion of neon atoms is created at this level, and their subsequent transition from the metastable level to a lower one is accompanied by the emission of photons with a wavelength of $\lambda = 632.8$ nm. It should be noted that the photon generation occurs also at wavelengths of 3.39 μm and 1.15 μm. For effective laser operation, they must be suppressed, which is carried out, for example, by selecting the reflection coefficients of mirrors.

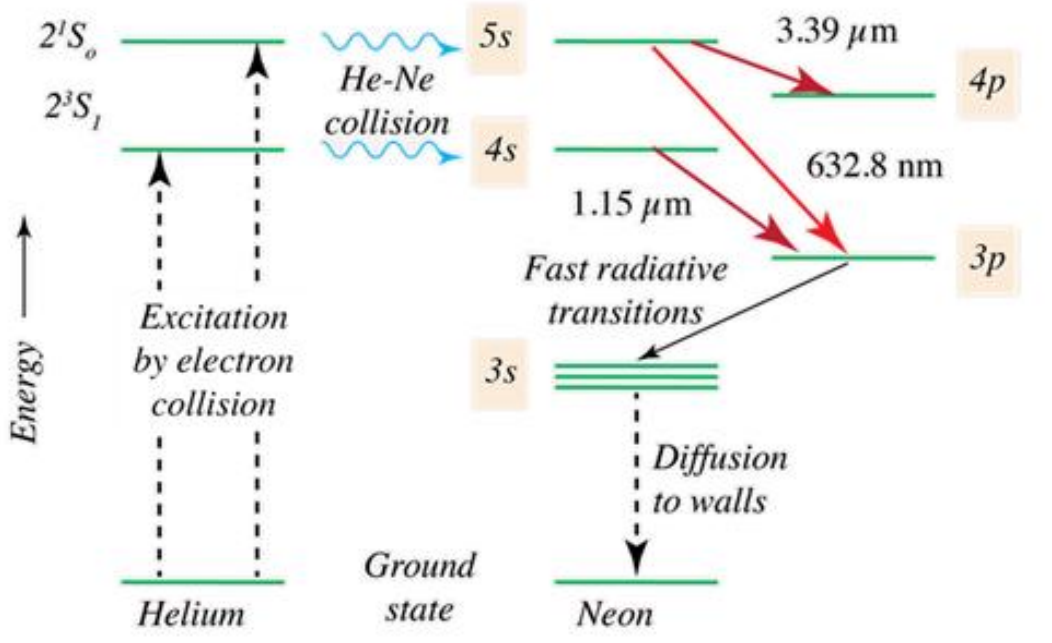

Fig. 14. Energy levels in He-Ne laser [30].

Photons emitted along the axis of the resonator are reflected from mirrors and repeatedly pass through the active medium, causing new acts of induced radiation. The result is coherent, monochromatic, directed radiation.

2.1.2. Spectrometer

There are two important types of spectrometers that are distinguished based on the system used to separate light into its components: dispersive spectrometers using a diffraction grating and Raman spectrometers with Fourier transform using a Michelson interferometer. These two types of spectrometers fundamentally differ in the physical principles underlying their design [15].

2.1.2.1. Raman dispersion spectroscopy

The Raman dispersive spectrometer usually uses lasers in the visible range. Typical laser wavelengths are 785, 633, 532, and 483 nm. Dispersive Raman spectrometers are based on classical optical schemes of monochromators, in which high-quality diffraction gratings with different number of strokes per mm are used as dispersing elements. According to their design features, Raman dispersive spectrometers can be divided into two categories.

The first category includes traditional dispersive Raman spectrometers built on either double or triple monochromators [7]. The design of optical circuits of such devices is based on the schemes of monochromators with either subtraction or addition of dispersion. Using the dispersion subtraction scheme minimizes the level of scattered light, which allows one to obtain high-quality Raman spectra in the low-frequency region of the spectrum (from 3 cm^{-1}). At the same time, using a scheme with the addition of the dispersion makes it possible to realize the maximum resolution of the system. These two schemes do not exclude, but mutually complement each other [31]. An example of the optical scheme of a double monochromator with subtraction is shown in Fig. 15. Optical components 1-6 and 14 belong to the first monochromator, optical elements 8-12 belong to the second monochromator. The spectral slit 7 is the output slit of the first monochromator and simultaneously the input slit of the second. This slit is called the intermediate.

Devices of the first category are usually used for solving complex fundamental problems that require high accuracy and the best metric characteristics. Working on devices of this type requires high scientific qualifications.

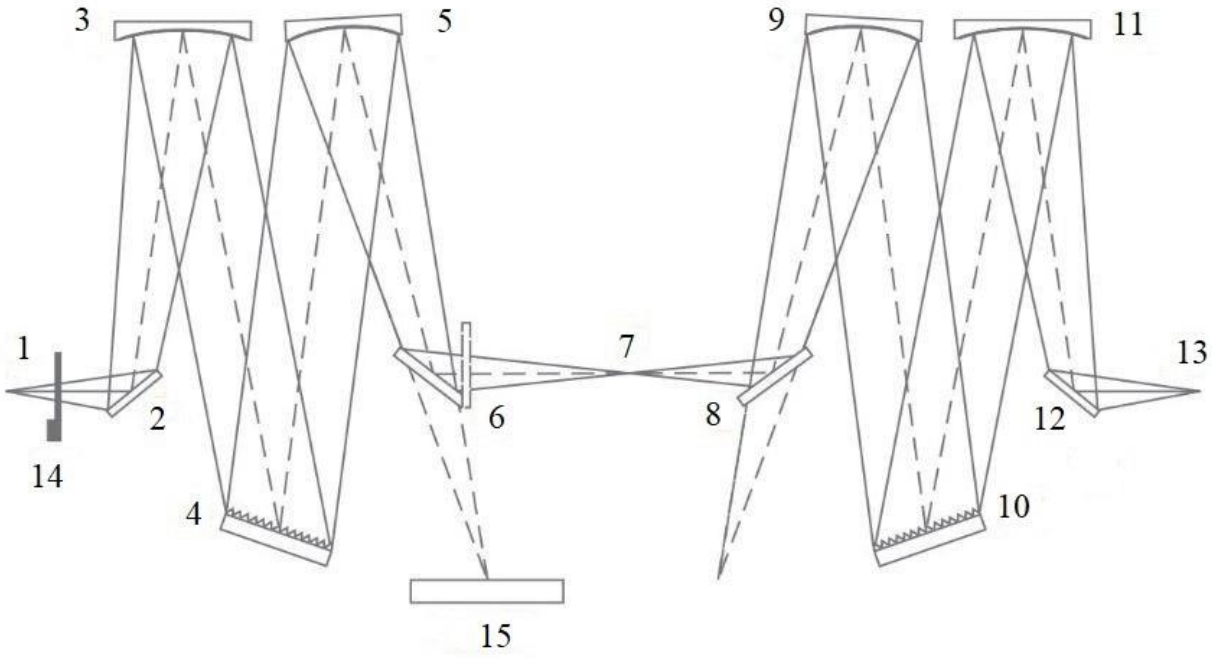

Fig. 15. Optical scheme of a double monochromator with subtraction. Designations: entrance slit (1), input rotary mirror (2), collimating mirror (3 and 9), diffraction grating (4 and 10), camera mirror (5 and 11), automated rotary mirror (6 and 8), intermediate slit (7), output rotary mirror (12), exit slit (13), light shutter (14), and CCD (15) [31].

The second category includes dispersion type devices in which the optical scheme is based on a single monochromator. An example of the structure of such a monochromator is the Czerny-Turner construction (Fig. 16).

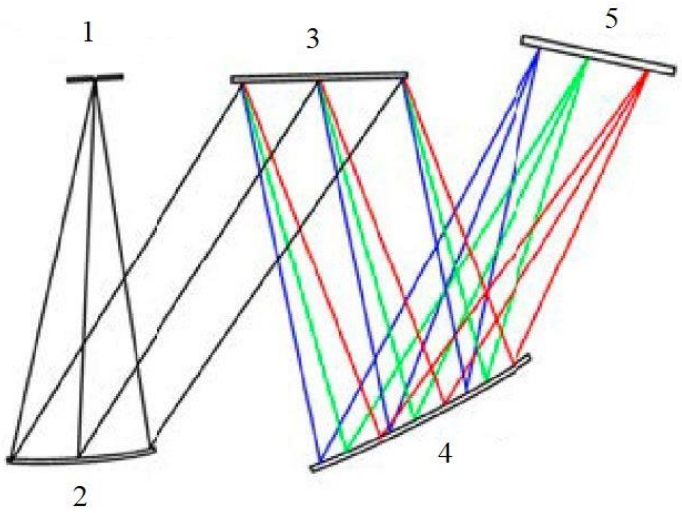

Fig. 16. Scheme of a single Czerny-Turner monochromator. Designations: entrance slit (1), mirror (2 and 4), diffraction grating (3), and CCD (5) [31].

The excitation laser line is cut off using special contrast filters (notch filters), which reduces the overall level of scattered light in the spectrometer. The use of such a scheme considerably increases the sensitivity of a device, but at the same time significant limitations arise when studying the low-frequency region of the Raman spectrum. In addition, each excitation laser line requires its own cut-off filters. Second category devices often approach the devices of the first category by resolution, since the resolution is largely determined by the quality of the diffraction grating, the number of strokes per mm. Modern instruments mainly use gratings with 1800, 1200, and 600 strokes per mm.

Devices of the second category are usually used for solving structural analytical problems. This, however, does not mean that they cannot be used to solve problems of a wide range of fundamental science. The operation of these devices does not require high scientific qualifications.

To register Raman spectra, the first category of spectrometers utilizes either cooled CCD detectors or, less commonly, cooled photomultipliers, while the second category of spectrometers uses only cooled CCD detectors.

2.1.2.2. Application of the dispersion Raman spectroscopy

Raman dispersion spectroscopy is used for the analysis of a wide range of samples. Lasers with shorter wavelengths and more sensitive CCD detectors make the method ideal for analyzing inorganic micro-components in solutions and composites [25].

The main applications of Raman spectroscopy with lasers in the visible region are semiconductors and electronics, where silicon and various coatings on silicon wafers are studied. Analysis of silicon products by Raman dispersion spectroscopy method provides information about the tensile stress and shear stress of silicon, as well as other important properties for the quality of the product [32]. Given the size reduction of silicon devices, the spatial resolution of dispersion spectroscopy is very important [6].

Raman dispersion spectroscopy is used also in pharmaceutical and biochemical studies [7]. This is due to the emergence of new research tasks, such as the study of single crystals and the mapping of biological tissues with high spatial resolution. Since these materials can fluoresce, a 785 nm laser is used as a rule.

Raman dispersive spectrometers are today the most versatile tools for structural spectral studies of various nanostructures, nanotubes, different modifications of sp^2 carbon, fullerites, graphites of various genesis, diamonds, both natural and artificial. In addition, dispersion Raman spectroscopy is widely used for inorganic analysis and identification in geology and gemology [10].

2.1.2.3. Raman spectroscopy with Fourier transform

Fourier transform Raman spectroscopy eliminates problems with the fluorescence of the samples, which is typical for dispersion Raman spectrometry. This is because Fourier transform Raman spectrometers use the excitation laser of 1 μm. In this case, the irradiation energy is reduced, and as a result, the probability of fluorescence is decreased.

The basis of Fourier spectrometers is a double-beam Michelson interferometer (Fig. 17), in which the path difference between the interfering rays changes when one of the mirrors is moved [33].

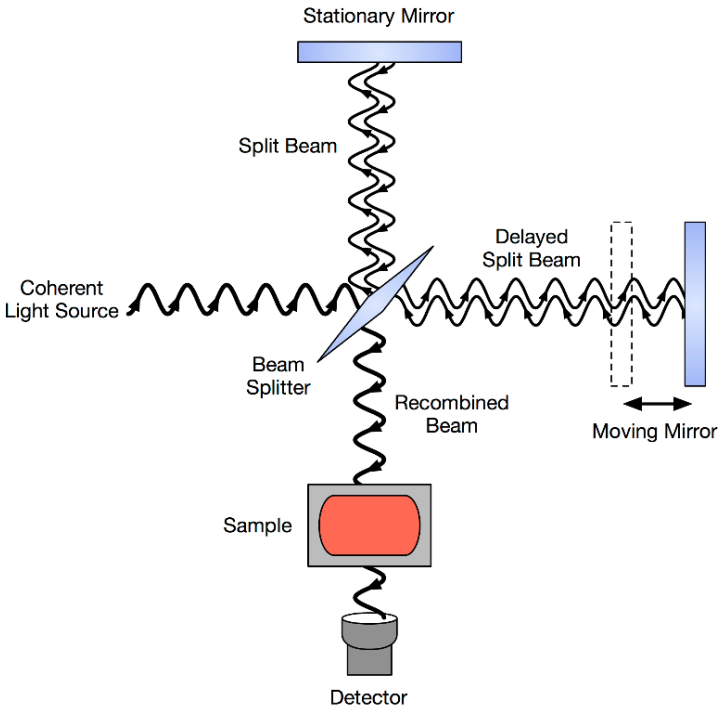

Fig. 17. Schematic diagram of the Michelson interferometer [34].

The interferometer works with a beam splitter that divides the incoming Raman radiation into two optical beams, one transmitted and one reflected. The latter is then reflected from the fixed flat mirror. The transmitted beam is reflected from a flat mirror, which is controlled by a movable mechanism; this mirror moves within a short distance (usually a few millimeters) from the beam splitter. These two beams are then recombined on the beam splitter, and due to the difference in the distances between the mirrors, the beams interfere with each other, resulting in a spectral band that is registered on the detector [7].

The resulting interferogram contains all information about the emission spectrum. The spectral resolution is determined by the distance over which the movable mirror moves. It should be noted that to obtain a spectral resolution of 10 cm^{-1}, a mirror movement of only one millimeter is

required. Such a movement can be carried out very quickly. That is, the obvious advantage of Fourier spectrometers is the high speed of spectrum registration. In contrast to the dispersive spectrometer, there are no slits that strongly diaphragm the beam. In the Fourier spectrometer, there is also no problem associated with the need to filter different orders of diffraction, which is typical for diffraction devices. The accumulation of interferograms, in contrast to the accumulation of spectra, can significantly increase the dynamic range of spectrum registration.

However, along with many obvious advantages of Fourier spectrometers compared to dispersion devices, there are also problems. Fourier transform spectrometers require very precise mirror movement, which implies appropriate mechanics and sophisticated mirror control systems. To obtain high-quality interferograms, optical elements must be of high quality. All this leads to the fact that existing implementations of devices are quite expensive and cover mainly the infrared range, where they simply have no competitors in spectral resolution and dynamic range [35].

2.1.2.4. Applications of Raman spectroscopy with Fourier transform

Raman Fourier spectroscopy is the best choice if the samples have fluorescence or contain micro-mixtures that can fluoresce. With great success, Fourier-Raman spectroscopy is used in the pharmaceutical analysis for the identification of unknown substances, analysis of raw materials, and qualitative and quantitative analysis of finished products. Fourier spectroscopy has an advantage in this area compared to dispersion Raman spectroscopy because pharmaceutical samples often have fluorescence when excited by a 785 nm laser, but give excellent spectra when excited by a 1000 nm laser.

For the same reasons, Raman spectroscopy with Fourier transform is widely used in forensic science for analyzing samples and physical evidence in sealed containers or packaging. In this case, the packaging does not need to be opened since the packaging does not contribute to the spectrum of the sample. Fourier-Raman spectroscopy is very useful when investigating illegal drugs, explosives, and fibers [36].

Pure polymers usually do not fluoresce, but micro-additives such as plasticizers have fluorescence when excited by a laser in the visible region [37]. Fourier spectroscopy is commonly used for most polymer samples. In addition, Raman spectroscopy with Fourier transform is widely utilized in chemical analysis of pulp, paper, textiles, and petrochemicals.

2.1.3. Detector

Silicon CCD (charge-coupled device) matrices are used to register Raman spectra. CCD is a specialized analog integrated circuit based on photodiodes. The extreme sensitivity to light makes these detectors suitable for analyzing a weak Raman signal [15].

The detecting surface of the CCD is a one-dimensional or two-dimensional matrix of light-sensitive elements, pixels. Each pixel works as an individual detector, so each scattered wavelength is detected by a separate pixel, or a closely located group of pixels (Fig.18).

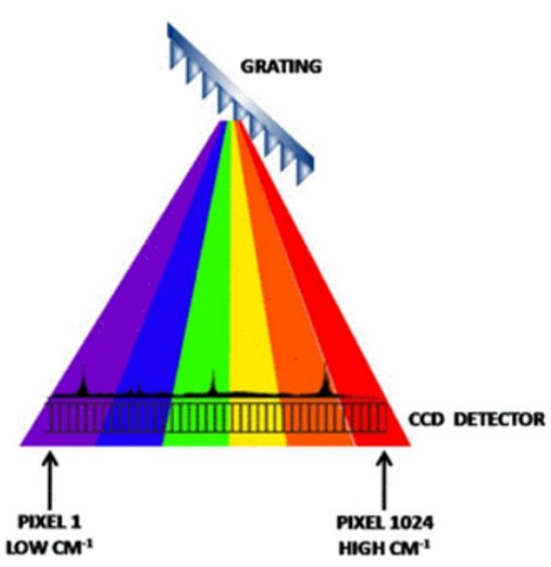

Fig. 18. Scheme of registration of the light dispersion spectrum by a CCD detector [38].

As already noted, the scattered light is dispersed by a diffraction grating in a typical dispersive Raman spectrometer. This dispersed light is projected onto the long axis of the CCD matrix. The first element detects light from the short-wavelength part of the spectrum (low cm^{-1}). The second element detects light from the next spectral position, and so on. The last element detects light from the long-wavelength edge of the spectrum (high cm^{-1}) [38].

The sensitive element of a silicon LED detector is a MOS capacitor that accumulates charge and discharges when light hits its light-sensitive surface. The accumulation of electric charge in the MOS capacitor occurs under the influence of photon "bombardment". The value of this charge is proportional to the intensity of the light flux and the time of its exposure. After the integration time has expired, the charge is buffered and transferred to the converter.

CCD detectors are capable of covering a wide range of spectra and provide a high resolution of the device. However, CCDs require a certain degree of cooling to make them suitable for proper operation. Cooling of CCD matrices is used to reduce dark noise [39].

The dark noise is caused by the presence of thermal electrons on the sensitive elements even in the absence of lighting, so the photodetector shows a weak signal. This effect is called the dark current. This current is constantly present on the CCD and interferes with long exposures on the matrix. Fig. 19 shows the dark noise for an uncooled and cooled CCD detector over an integration time of 60 seconds. When operating at room temperatures, dark noise is almost completely dissipated by the uncooled CCD detector. Once the CCD is cooled to 10°C, the dark current decreases approximately four times.

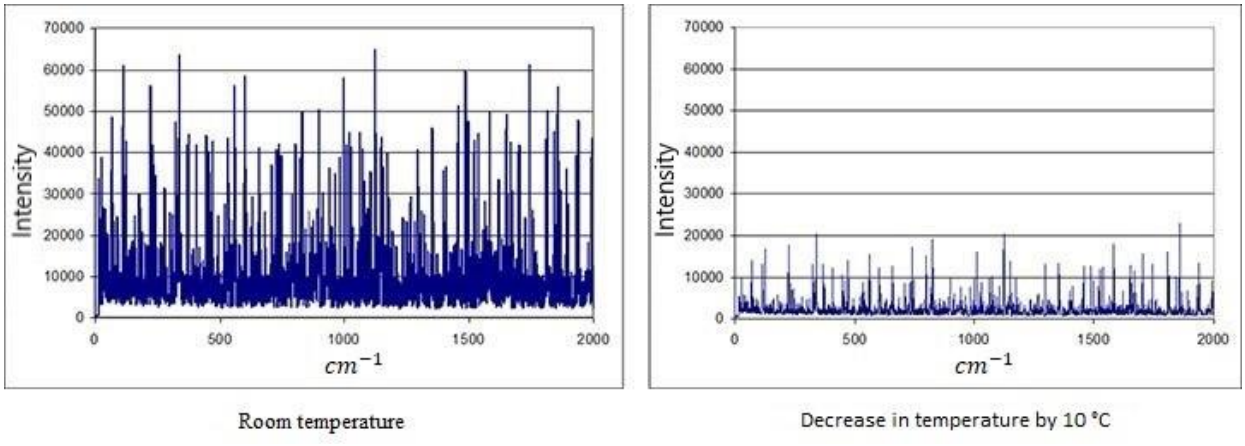

Fig. 19. Dark current for an uncooled and cooled CCD detector (integration time is 60 seconds) [31].

Cooling can be performed using a Peltier thermoelectric element or cryogenic cooling with liquid nitrogen. Most Raman systems use cooling by Peltier batteries, which are capable to provide a drop of 70°C. In addition, these batteries are so compact that they are mounted directly in the same housing together with the CCD crystal [40].

2.2. The principle of operation of the Raman spectrometer

Fig. 20 shows a schematic diagram of a typical Raman dispersive spectrometer.

The investigated sample is placed on a motorized stage with stepper motors. The stage can move over long distances, tens and hundreds of mm, with a minimum step of 50 nm. Some models of spectrometers use an alternative piezoelectric table; its operating range is only a few hundred micrometers. These piezoelectric tables can provide a nanometer step, which is incredibly important when studying nanoobjects such as carbon nanotubes and quantum dots.

In the entrance of the laser beam there is a system of filters to control beam intensity. This is necessary in order to prevent the heating and ignition of the test sample. Linearly polarized light,

passing through the lens system in the microscope objective, focuses on the sample surface. After interacting with the sample, the scattered light is collected by the same lens and the light passes through a notch or otherwise edge filter, which suppresses the exciting line (photons with a Rayleigh wavelength) and transmits only photons with a shifted wavelength value. The notch filter is chosen depending on the laser used and is determined by its wavelength [2].

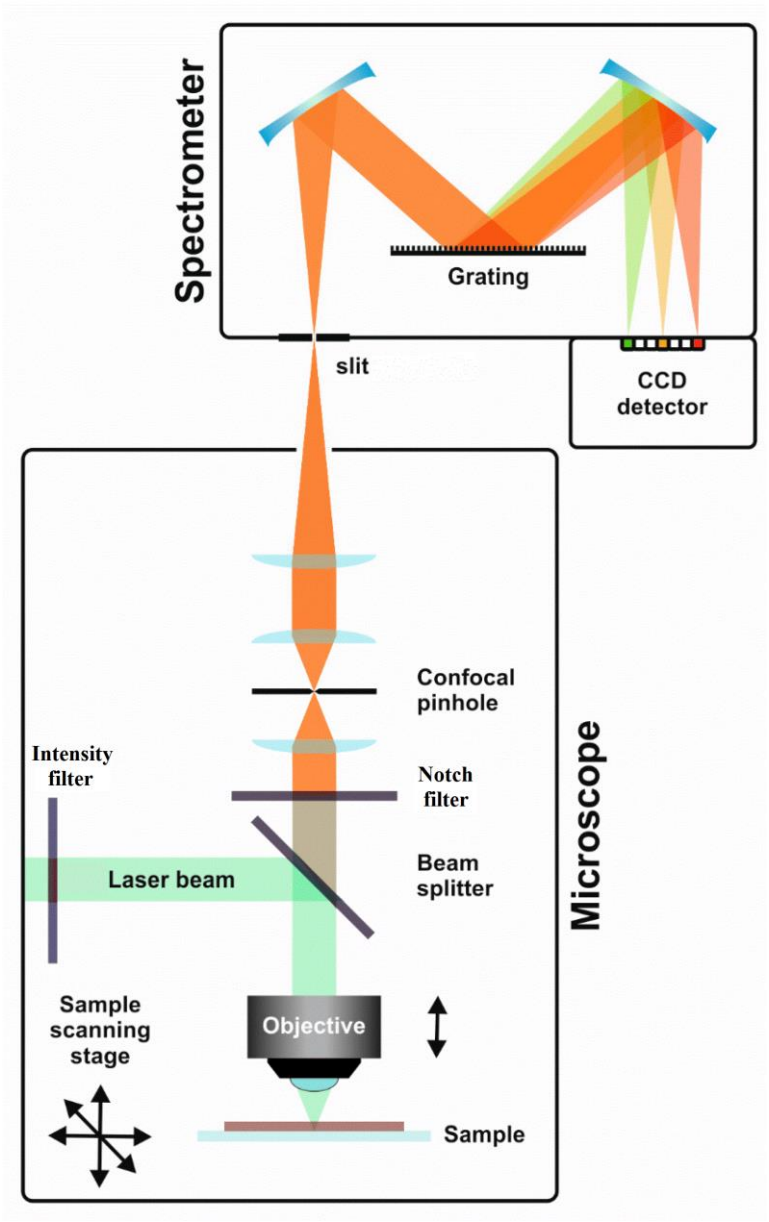

Fig. 20. Schematic diagram of the dispersive Raman spectrometer [41].

Next, the light beam is directed to a confocal aperture, which set to register light from only one point region. The confocal hole is a small diaphragm and is positioned so that the light emitted by the analyzed point passes through the diaphragm and will be registered, while the light from other

points will be delayed by the diaphragm. The diaphragm is implemented as a pinhole with an adjustable diameter (Fig. 21) [24, 42].

A positive consequence of using a confocal hole is a significant reduction in the focal length. This means that with confocal optics, it is possible to distinguish the signal from each layer of a multilayer sample or isolate the signal from extraneous sources located in the surrounding space.

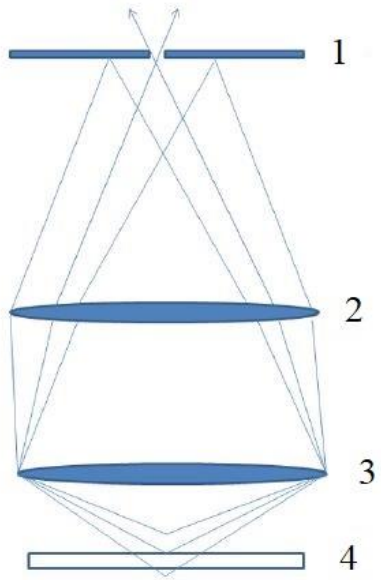

Fig. 21. Scheme of the confocal optical system. Designations: confocal hole (1), lens (2 and 3), sample (4) [43].

The performance of the spectrometer depends on the confocal aperture since it directly affects the light flux going to the optical part. The optical resolution and bandwidth of the spectrometer are completely dependent on the size of the hole. The smaller the confocal hole, the better spectral resolution. But at the same time, the total intensity of the light passing through the confocal system also falls (Fig. 22), so confocality is always a compromise between signal power and resolution [43].

After passing through the confocal hole, the light beam is transported using a system of mirrors and lenses and directed to the entrance slit in the spectrometer. The functional load of this slit is similar to the confocal hole - the entrance slit controls how much light enters the spectrometer. The size of the slit affects the resolution: the narrower it is, the higher the resolution. However, narrower slits also reduce signal strength. These two factors must be balanced when choosing the slit size.

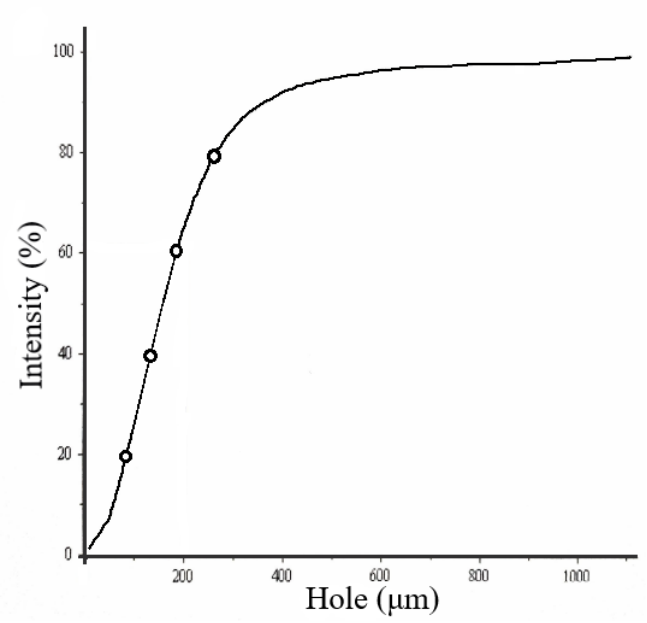

Fig. 22. Relationship between the aperture of the confocal hole and the signal intensity [43].

Light passing through the diffraction grating in the spectrometer is decomposed into components, and then it is directed to a detector. The CCD matrix, depending on the incidence point coordinate of the beam on the matrix, associates a certain wavelength or frequency and corresponding intensity. From the CCD detector, the received information sends to the computer, where the system forms the spectrum.

RAMAN EXPERIMENT

3.1. Experimental equipment

To investigate the operation principle and to perform experiments, the Raman spectrometer LabRam HR800 of Horiba Jobin-Yvon Company was used (Fig. 23). It is a dispersive spectrometer with a single monochromator and is characterized by the following features [43]:

- wide spectral range

The spectral range of the device is within 65…4000 cm^{-1}, using the excitation line of the He-Ne laser 633 nm. The design of the spectrometer makes it easy to switch from one spectral range to another by replacing the diffraction gratings. Despite the complexity of the optical scheme, this replacement does not require a complicated additional adjustment of the device.

- high resolution

The device gives a resolution of about 0.5 cm^{-1}. The resolution is the determining parameter when studying contours and FWHM in the Raman spectra.

- accuracy of detection and reproducibility of wavelengths

The accuracy and reproducibility of wavelengths are of great importance for precision studies of the FWHM, contours, and position of the spectrum lines. This parameter is 0.8…1 cm^{-1}.

- low level of scattered light in the device, the ability to explore the low-frequency region of the spectrum (spectrum of lattice vibrations)

The ability to study the phonon spectrum in the region of 65…1000 cm^{-1} allows one to obtain direct structural information about the crystalline state of a matter and to study phase transitions and polymorphism in crystals.

- confocal optics

The presence of confocal optics makes it possible to analyze the surface of the test sample and to obtain a Raman signal from an area of 100 microns. In addition, confocal optics improves resolution and allows the analysis of complex microregions.

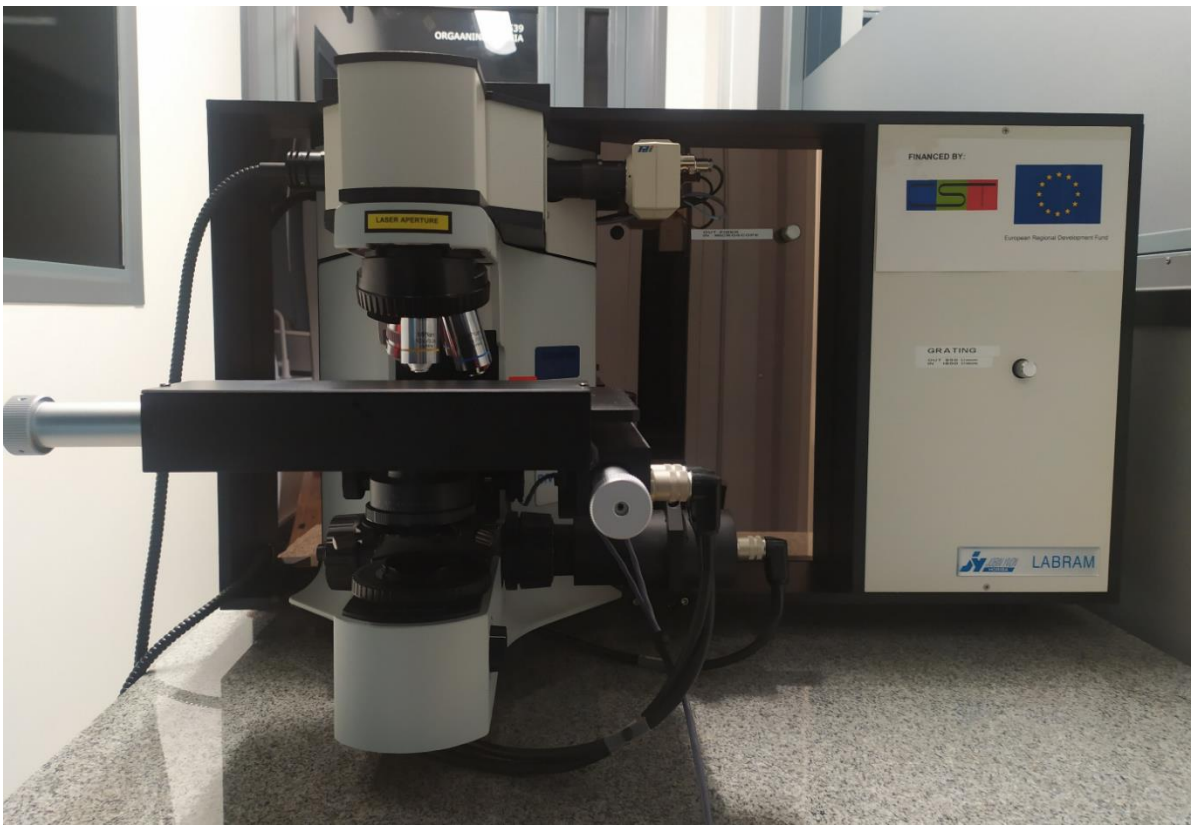

Fig. 23. Raman spectrometer Horiba Jobin-Yvon LabRam HR800.

3.1.1. Software

The LabSpec program is used for obtaining, analyzing, and processing spectra. The main program window consists of the main menu, toolbar, workspace, instrument settings, and temperature indicator of the CCD matrix. The interface of the LabSpec program is shown in Fig. 24.

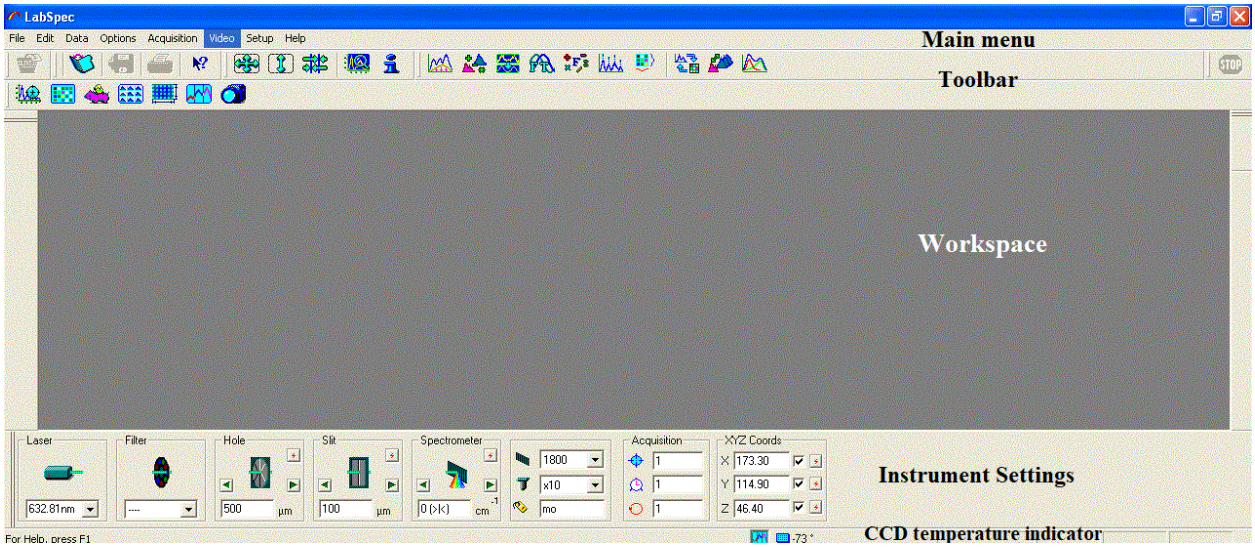

Fig. 24. The interface of the LabSpec program.

3.1.2. Selecting the operating parameters of the spectrometer

Consider in detail operator-configurable instrument parameters; most of them are presented at the bottom of the LabSpec window (Fig. 25).

- spectral frequency range (cm^{-1})

As a rule, the range of 100-1000 cm^{-1} is chosen for the study of crystal lattices, and values of more than 1000 cm^{-1} are taken for molecules. This division is conditional and often there is a need to study the spectrum in the entire available range. Selecting a wider range increases the time it takes to get the resulting spectrum, therefore, if one knows the limits within which peaks are expected to be registered, the spectral frequency range should be limited.

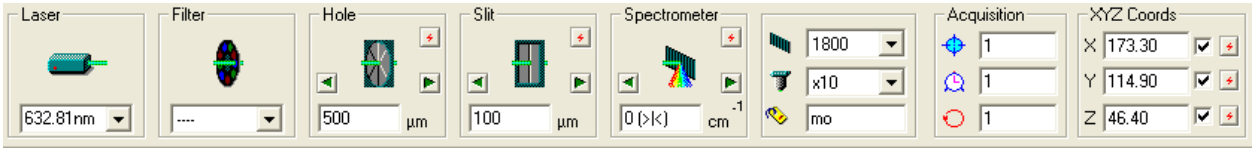

Fig. 25. Operator-controlled parameters that influence spectrum formation.

- laser

The spectrometer has two laser light sources - internal and external. The internal He-Ne laser with a wavelength of 633 nm and a power of 20 mW is built into the housing and is located at the rear of the device. There is also an external laser with a wavelength of 785 nm. The design of the device gives the possibility of replacing the external laser with any other, wavelength of which in the range of 440-800 nm.

When replacing a laser, it is necessary to make sure that notch filters, specific to a given radiation source, are installed in the optical system as well as adjusting the position of a special mirror (up or down). Each time the laser is replaced, this must be done manually (Fig. 26).

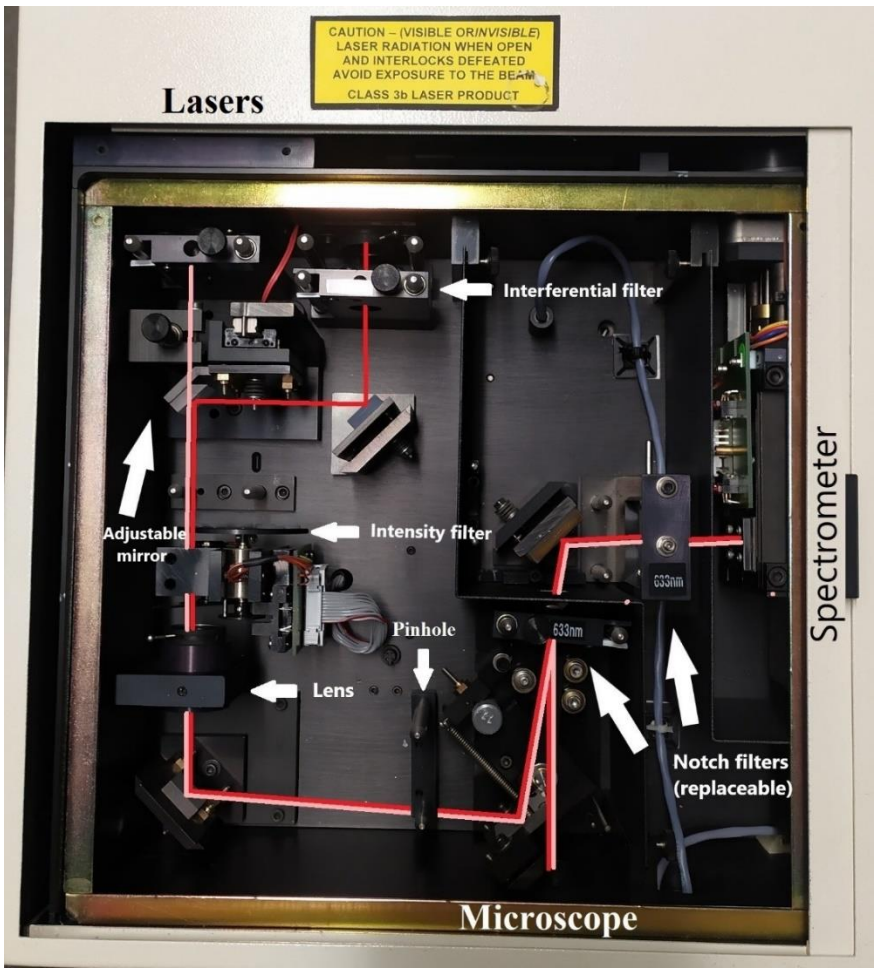

Fig. 26. The optical system of the device. Red color indicates the path of the beam from the external laser, pink color from the internal laser.

- filter

In order to prevent heating and ignition of the sample, a filter that controls the radiation intensity is installed in the path of the laser beam. The operator in the program can choose one of six possible filter options, characterized by the following optical densities:

[...] = no attenuation (I_0)

[D0.3] = $I_0/2$

[D0.6] = $I_0/4$

[D1] = $I_0/10$

[D2] = $I_0/100$

[D3] = $I_0/1000$

[D4] = $I_0/10000$

The process of changing the intensity filter is automated. Fig. 27 shows the spectra obtained for mica sample in the absence of a filter, with the filter [D0.3] and [D0.6]. It can be seen from the intensity values of the spectrum peaks that the filters fully correspond to the declared optical densities.

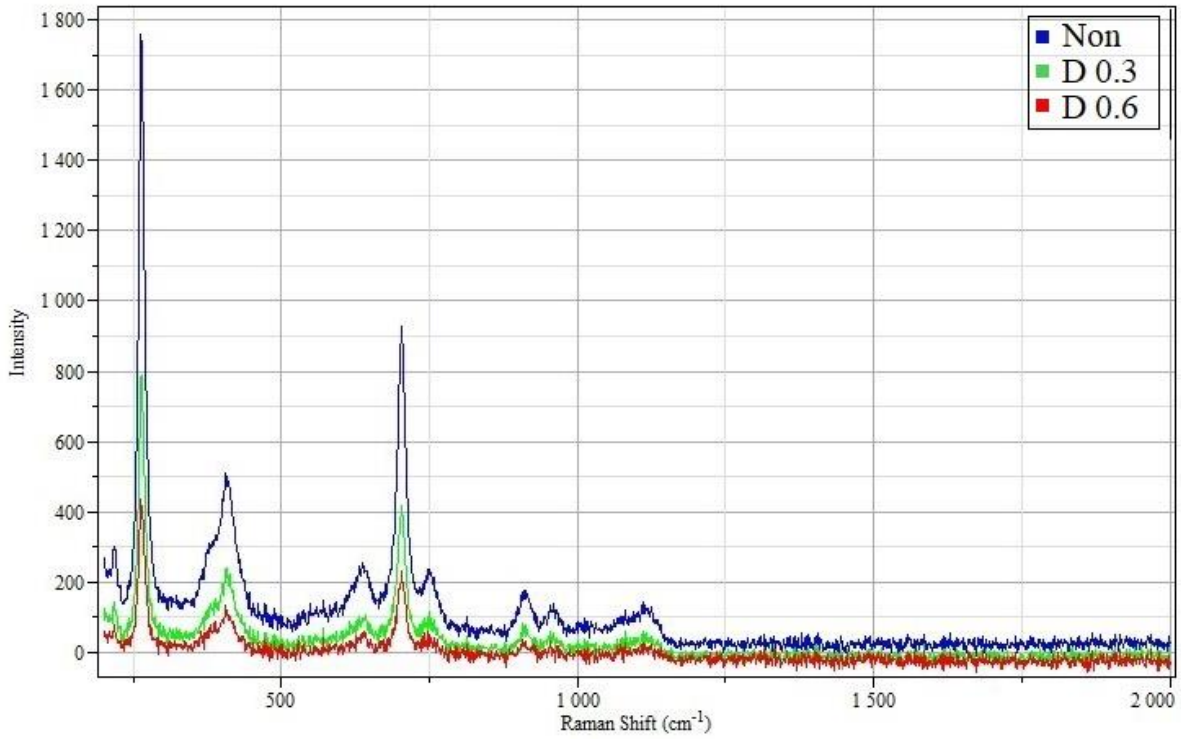

Fig. 27. Comparison of mica spectra obtained without a filter, with the filter [D0.3] and [D0.6]. The spectrum was obtained with an exciting line of 632.8 nm, a confocal hole of 500 μm (H=500 μm), and an entrance slit in the spectrometer of 100 μm (S=100 μm).

- confocal hole

As already noted, the width of the confocal hole directly affects the size of the light flux transfers to the optical part. As the confocal hole increases, the signal value increases as well (Fig. 28). The hole size can be set in the range from 0 μm to 1500 μm.

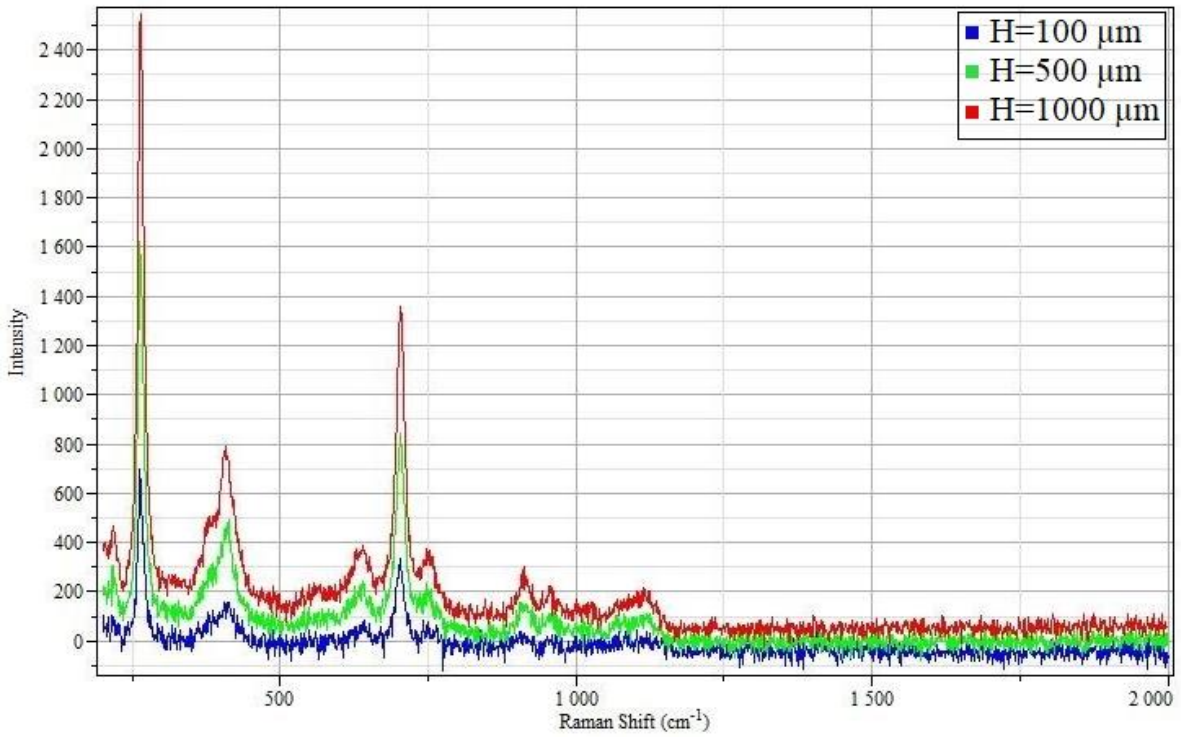

Fig. 28. Comparison of mica spectra at different confocal hole values H=100 µm, H=500 µm, and H=1000 µm. The spectra were obtained with an exciting line of 632.8 nm, S=100 µm.

- slit in the spectrometer

The entrance slit in the spectrometer performs the same functions as the confocal hole, it controls how much light enters the spectrometer. Accordingly, the effect of the enterance slit width on the signal is similar.

- diffraction grating

The diffraction grating forms a spectrum of light and affects the optical resolution of the spectrometer. The higher the density of strokes of the diffraction grating, the greater the dispersion angle is observed (Fig. 29). When the dispersion is doubled, the integrated signal becomes about half as small, because each pixel registers only half of the number of photons passing through the diffraction grating.

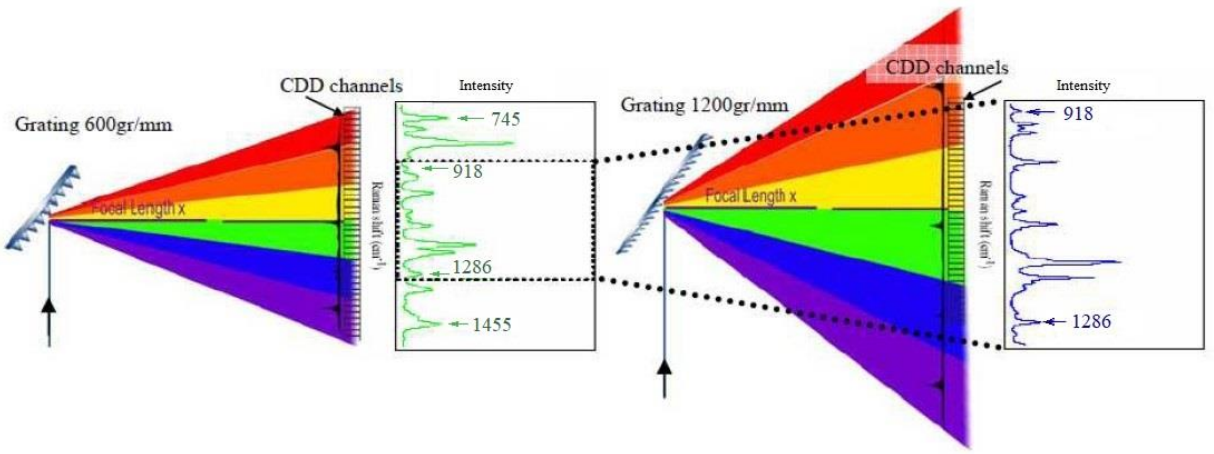

Fig. 29. Influence of the diffraction grating on the Raman spectrum [38].

At the same time, diffraction grating with a higher density of strokes make it possible to distinguish closely located peaks and peaks of weak intensity (Fig. 30). As a result, the spectrum is more clear and precise.

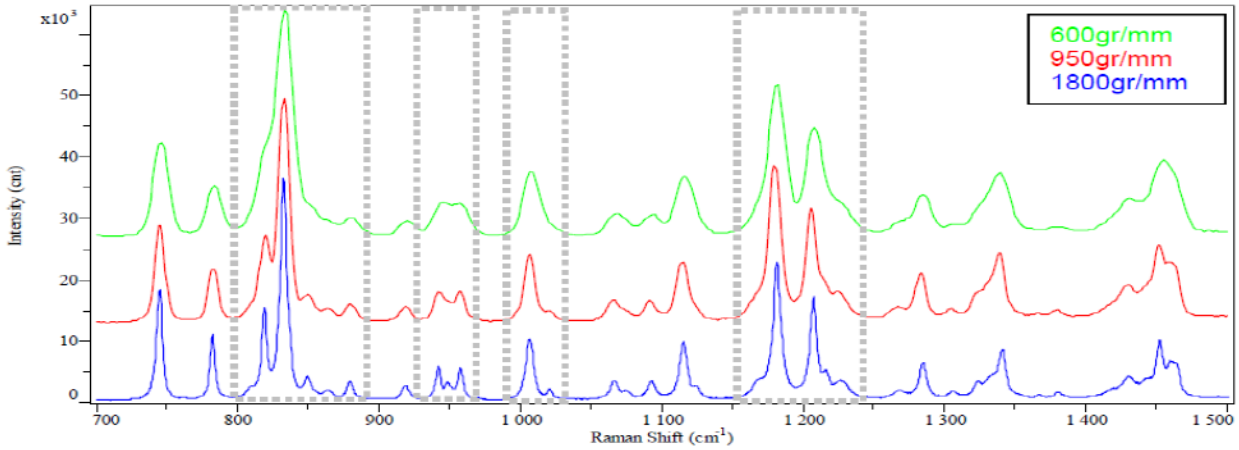

Fig. 30. Spectrum shape when using different diffraction gratings [38].

There are two diffraction gratings available in the present spectrometer LabRam HR800, namely 1800 mm^{-1} and 900 mm^{-1}.

- objective

The installation uses lenses with magnification x10, x50 and x100. Obviously, a larger magnification allows one to focus more precisely on a specific area of the sample, which is

extremely useful, for example, in the case of multicomponent material. Besides, when choosing a lens, it is necessary to take into account the transparency of the sample.

Opaque sample

If the laser beam practically does not penetrate the sample, the Raman spectrum is determined to a greater extent by the surface of the material; and its intensity is proportional to the reflected flux. Strictly speaking, the intensity of the scattered signal is proportional to the square of the numerical aperture (3) [43].

The numerical aperture depends on the aperture angle and is found according to the formula:

$$NA = n * \sin \alpha, \quad (3)$$

Where n is the refractive index of the medium between the test sample and the lens, and α is the angle of aperture.

The aperture angle (beam divergence angle) in laser physics is defined as the angle between the axis and the set of points of the laser beam at which the radiation intensity drops to e^{-2} times in comparison with the intensity on the axis (Fig. 31).

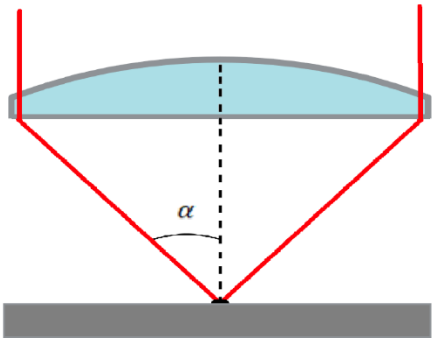

Fig. 31. Aperture angle of the laser-focused beam.

Second important characteristic of the lens that determines its resolution is the maximum diameter of the illuminated spot:

$$T = 1.22 * \frac{\lambda}{NA}, \quad (4)$$

Where λ is the wavelength of the exciting laser, and NA is the numerical aperture of the lens.

Thus, in the case of an opaque sample, it is more appropriate to use a microscope objective with a higher magnification factor (100x) to have a larger aperture angle and obtain a better resolution (table 1).

Objective	α, °	NA	$(NA)^2$	T, μm
100x	64.2	0.90	0.81	0.96
50x	48.6	0.75	0.5625	1.03
10x	-	0.25	0.0625	3.1

Table 1. Optical characteristics of objectives with 100x, 50x, and 10x magnification. The data correspond to an exciting line of 632.8 nm, a confocal hole of 400 μm, and an entrance slit in the spectrometer of 100 μm [43].

Transparent sample

When using a transparent homogeneous sample, it is better to use a microscope objective with a smaller magnification (10x), since such lens allows one to collect a signal from a larger sample volume.

In addition to the considered structural elements, the Raman spectrometer has another important component, the shutter. It defines the following two parameters.

- exposure time

The exposure time is the period over which the shutter opens and the Raman signal affects the CCD matrix. The longer the exposure time, the more intense the analyzed spectrum. The parameter can vary from 0.000001 seconds to three days (259 200 seconds).

- accumulation number

This parameter determines the number of times the shutter opens. After collecting information, the program automatically calculates the signal intensity value by averaging the accumulated spectra. This allows one to increase the signal-to-noise ratio and remove the influence of cosmic rays that distort the spectrum. Cosmic rays are a component of natural radiation on the Earth's surface and in the atmosphere.

The X, Y, and Z values in the lower-right part of the LabSpec window (Fig. 24 and Fig. 25) indicate the current position coordinates of the stage.

3.2. Calibration of the Raman spectrometer

Before using the spectrometer and performing experiments, it is necessary to calibrate the instrument, since due to the presence of electronic and precision optical devices, the readings of the instrument may change over time under the influence of changes in the environment. Factors affecting the operation of the spectrometer include changes in temperature, humidity, pressure, mechanical stress, and so on.

The instrument is calibrated by the reference value of crystalline silicon peak (520.7 cm^{-1}). It is necessary to ensure that the peak position differs by no more than 2 cm^{-1} from the reference value. The spectrum of the calibration sample is shown in Fig. 32.

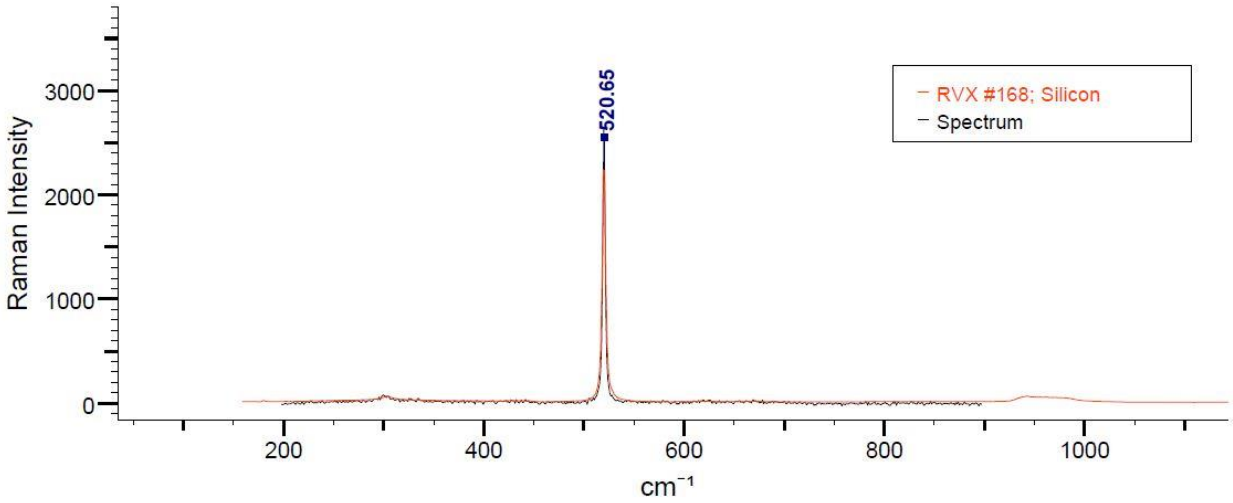

Fig. 32. Raman spectrum of crystalline silicon (Si). The black curve indicates the spectrum obtained, the red curve indicates the spectrum from the database. The spectrum was obtained with an exciting line of 632.8 nm, a confocal hole of 500 μm (H=500 μm) and an entrance slit of 100 μm (S=100 μm).

Determination of the chemical composition of a sample based on the obtained spectrum is performed using special software that includes extensive databases of spectra, ranging from simple substances to complex composite materials. In the present work was used the KnowItAll ID Expert software from Bio-Rad.

The analysis process involves comparing the parameters of the studied spectrum with database spectra and returning a list of identical substances with a percentage probability. Each of the possible options is accompanied by information about the chemical composition and characteristic properties (Fig. 33). Thus, several options of the chemical composition may correspond to the

studied spectrum. The final decision on the identification of the sample remains with the researcher. In this case, it seems appropriate to be based on known data about appearance, state of aggregation, and demonstrated properties.

Name	Value
Resulting HQI	99.40
Database Abbreviation	RVX
Database Title	Raman - Semiconductor Materials - HORIBA
Record ID	168
Name	Silicon
Classification	IV element
Comments	Eg=1.12eV indirect; k=11.9; penetration depth: ~ 3000nm for 632.8nm; spectrum without artefacts, large band ~ 1000 cm-1 is the second order Raman
Formula	Si
InChI	InChI=1S/H4Si/h1H4
InChIKey	BLRPTPMANUNPDV-
Instrument Name	HORIBA LabRAM
Raman Laser Power	632.8 mW
Sample Description	cubic - diamond type
Source of Sample	Jobin Yvon
Source of Spectrum	HORIBA Scientific

Fig. 33. Information displayed by KnowItAll ID Expert program about a substance using crystalline silicon Si as an example. HQI is the percentage probability of coincidence of the spectra.

After successful calibration of the device, one can proceed directly to measuring the spectra of the samples.

3.3. Obtaining Raman spectra of materials

One of the goals of this work was to verify the correct operation of the LabRam HR800 Raman spectrometer. For this purpose, four well-known samples was used, namely mica, paraffin, and two similar polymeric materials (polyethylene and polypropylene).

As already established, the optimal material for the substrate is foil, introducing the minimum background signal in the researching of transparent substances. Therefore, when studying the spectra of mica and polypropylene, the glass slide was wrapped with aluminum foil. The spectrum of such a substrate is shown in Fig. 34.

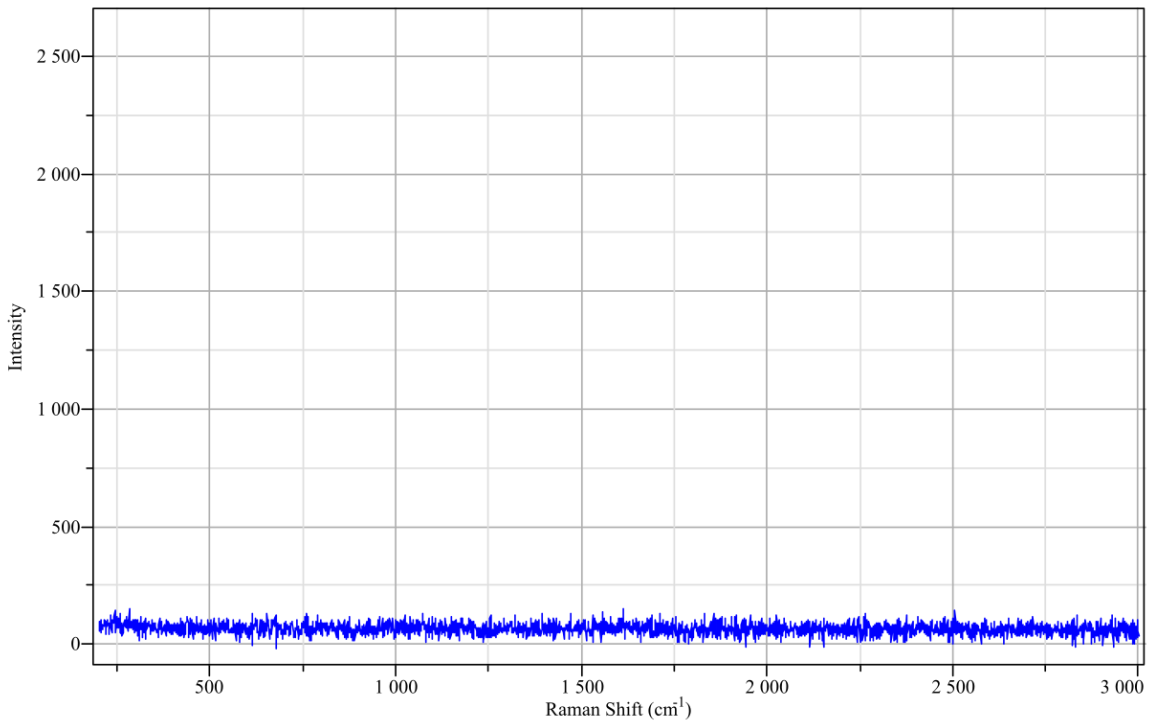

Fig. 34. Raman spectrum of aluminum foil. The spectrum was obtained with an exciting line of 632.8 nm, H=500 μm, and S=100 μm.

All investigated samples were determined with high accuracy; the probability of coincidence, so called HQI number (Fig. 33), was 97-99%. The spectra of all four samples are shown in Fig. 35.

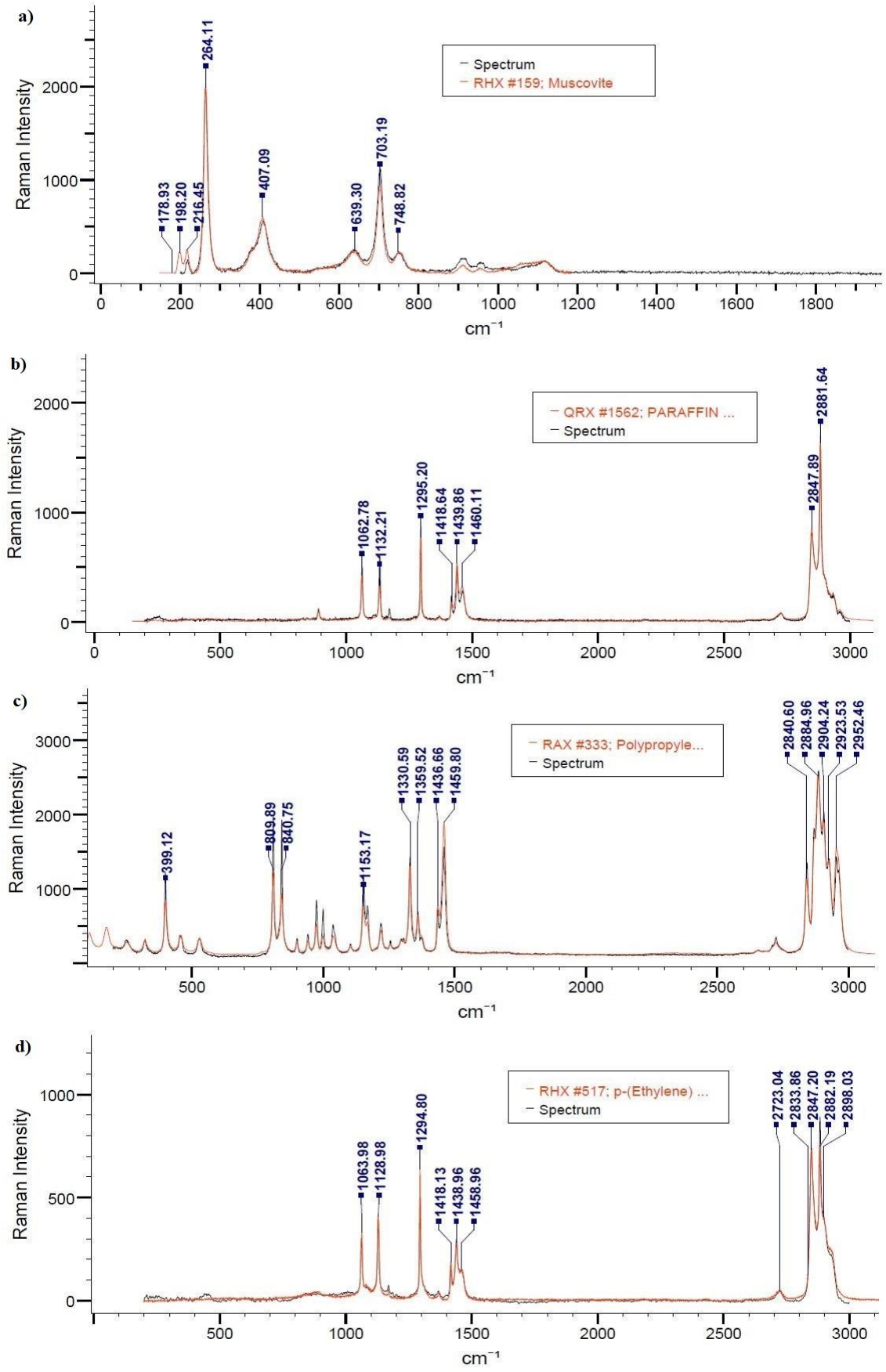

Fig. 35. Raman spectra of a) mica ($KAl_3Si_3O_{10}(OH)_2$); b) paraffin (C_nH_{2n+2}); c) polypropylene ($(C_3H_6)_n$); and d) polyethylene (C_2H_4). These spectra were obtained with an excitation line of 632.8 nm, H= 500 μm, and S=100 μm.

3.4. Raman spectral imaging of a surface

Raman mapping is a powerful tool for creating detailed images of the chemical structure of a sample surface based on its Raman spectra [4, 8]. The full Raman spectrum is measured for each point in the studied area, then the composition or structure of the material is identified from the spectrum, and the map is accordingly colored in different (artificial) colors for easy visualization. A color palette and brightness scale are used to visualize the Raman surface map, which makes it possible to display point-by-point chemical or structural properties. Accordingly, a change in the brightness of a pixel in the image corresponds to a change in the peak intensity at a given point, and a change in color indicates a change in its position or width.

Raman image mapping can be performed on all three coordinates (X, Y, Z), in any combination of them. Perhaps the most common is 2D mapping along the surface (XY plane), but other options are also very useful, such as 1D depth profiling (Z-axis), 2D optical vertical cross-section (XZ and YZ planes), and finally full 3D volume mapping (XYZ). To create a Raman spectral map, it is necessary to select the boundaries of the scanning area on the sample surface, as well as determine the resolution of the map, meaning the number and size of points at which the spectrum will be measured.

To study the surface and to obtain a Raman map, a cellulose filter was used, through which a control volume of water from a contaminated source had previously been passed. The task was to find microplastic particles on the filter surface to determine the presence of these substances in the aqueous medium under study.

First of all, analysis of pure filter was carried out to obtain the spectrum of this material (Fig. 36). This is necessary in order to subtract this spectrum from the Raman map of the contaminated sample and to exclude the influence of the substrate on the Raman signal.

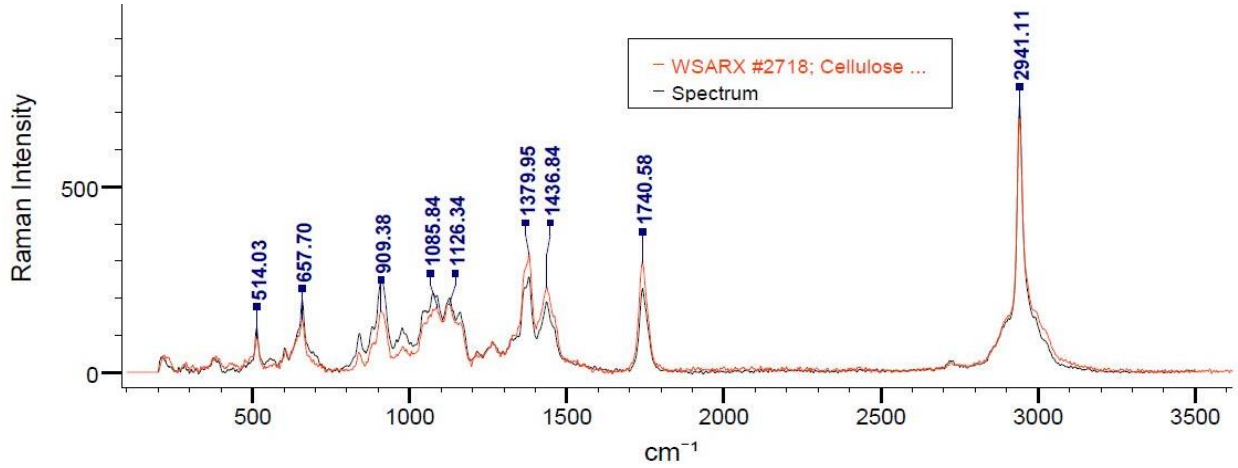

Fig. 36. Raman spectrum of a pure cellulose substrate ($C_{28}H_{38}O_{19}$). The spectrum was obtained with an exciting line of 632.8 nm, H=500 μm, and S=100 μm.

The mapping procedure is fairly a lengthy process. It takes approximately three days of continuous measurements to create a spectral map of an area of about 1 mm^2 and a number of pixels of about 8300 with a selected wavenumber range of 100-3000 cm^{-1}. Immediately after the measurements are completed, the program gives a spectral map showing the average signal intensity at each point (Fig. 37). White pixels correspond to the maximum Raman signal, while black pixels correspond to the minimum signal.

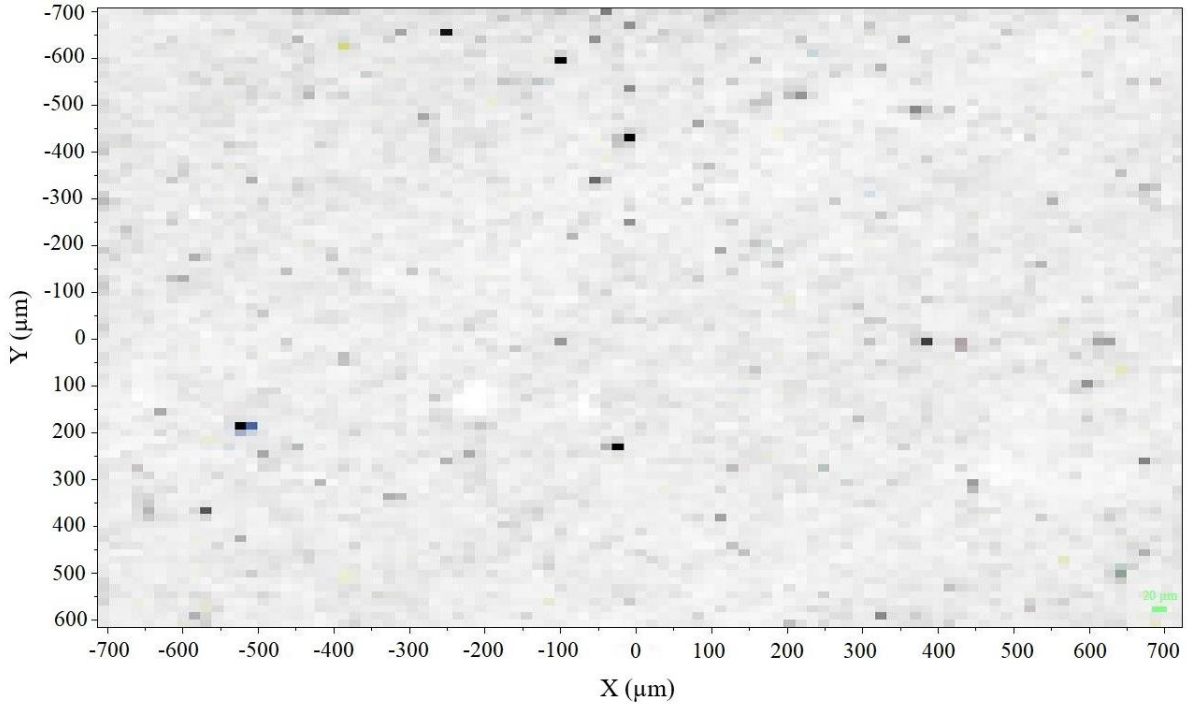

Fig. 37. Raman Spectral map of the surface of a contaminated filter.

In addition, the program calculates the total spectrum of the surface, representing averaging over all the obtained spectra (Fig. 38).

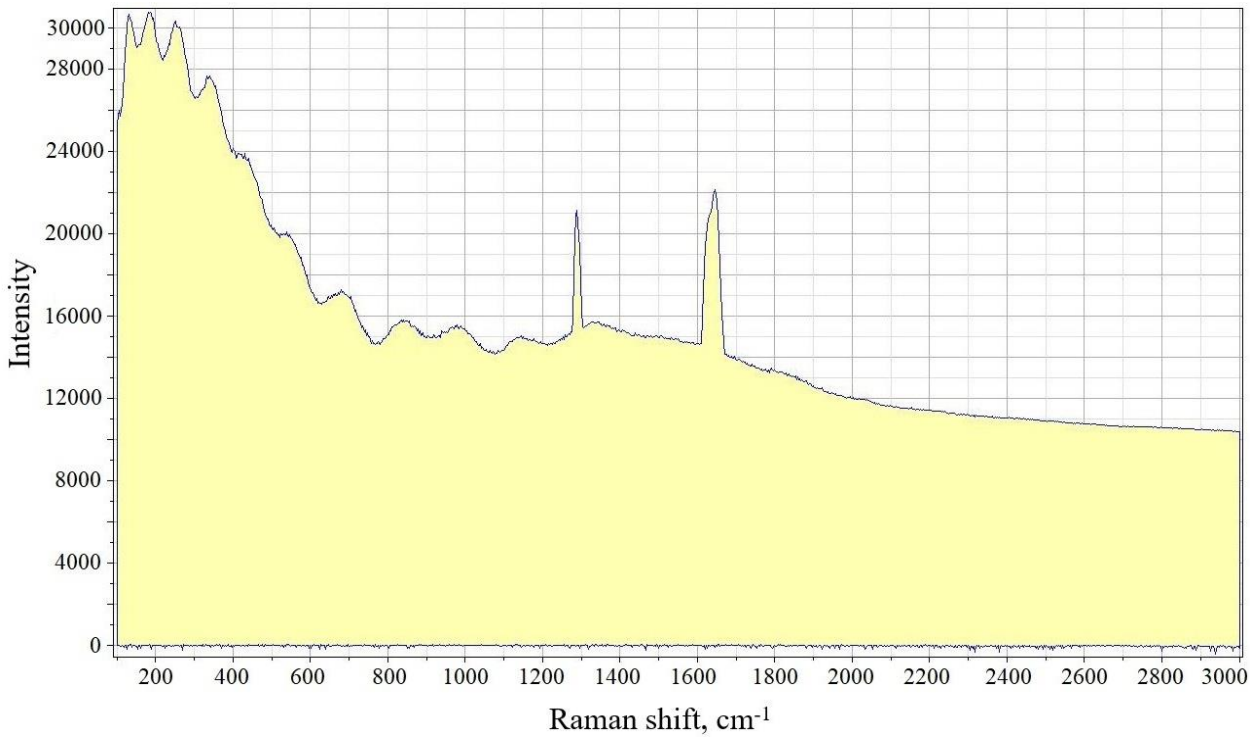

Fig. 38. The total average Raman spectrum of the filter surface. The spectrum was obtained with an exciting line of 632.8 nm, H= 500 μm, and S=100 μm.

The obvious result is the presence of suppressive fluorescence, due to the fact that the filter was in an aqueous medium with a large number of organic molecules. On the general spectrum, fluorescence is expressed in characteristic high signal intensity and the absence of clear peaks. On the spectral map, the fluorescent regions are marked with white pixels. Generally, even the presence of several fluorescent points on the surface would make a significant contribution to the overall spectrum, since, as mentioned earlier, fluorescence increases the signal intensity several tens of times (Fig. 39).

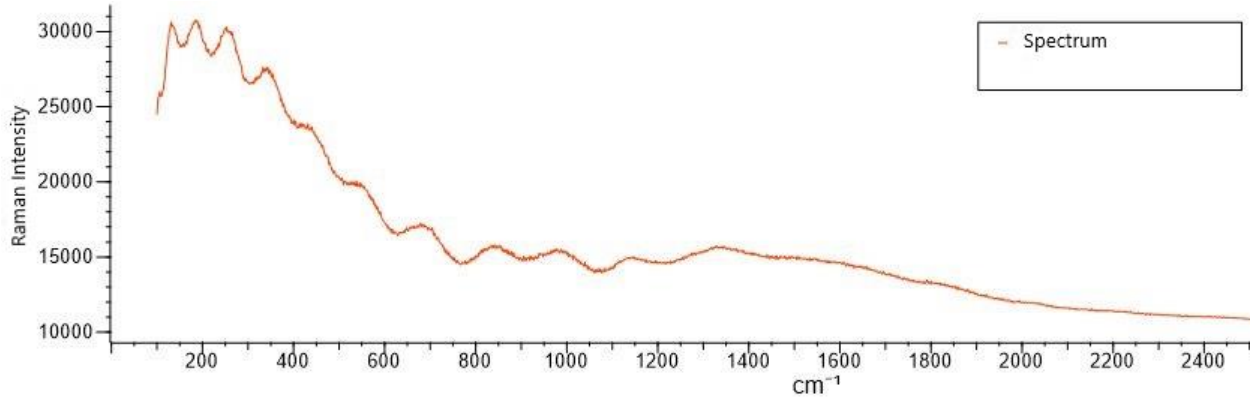

Fig. 39. Spectrum of the highly fluorescent region of the contaminated filter. The spectrum was obtained with an exciting line of 632.8 nm, H=500 μm and S=100 μm.

However, despite this, two relatively narrow peaks at about 1300 and 1650 cm^{-1} are clearly visible in the overall spectrum. These areas are of particular interest and will be discussed in more detail.

It should be noted that analysis based only on the total surface spectrum is not very indicative. In the presence of fluorescence, it is practically not possible to detect any substances. In the absence of fluorescence, it can show peaks corresponding to the predominant components on the surface, but important information about rare substances will not be displayed. Therefore, it is necessary to examine all the spectra registered by the system to determine the full chemical composition of the studied area.

The search for "pure" spectra without fluorescence can be done manually by examining the spectrum of each pixel in the map. This approach is possible only with a small number of points. With a high pixel density, this is impractical in view of the time costs and errors associated with the human factor. In this case, it is more reasonable to perform the analysis by highlighting certain ranges on the general spectrum and modifying the spectral map based on the signal intensity in a particular selected region of wavenumbers. In our case, the peaks of interest are located in two ranges: 1250-1350 cm^{-1} and 1575-1700 cm^{-1}. The green borders indicate the first range and the red borders the second (Fig. 40).

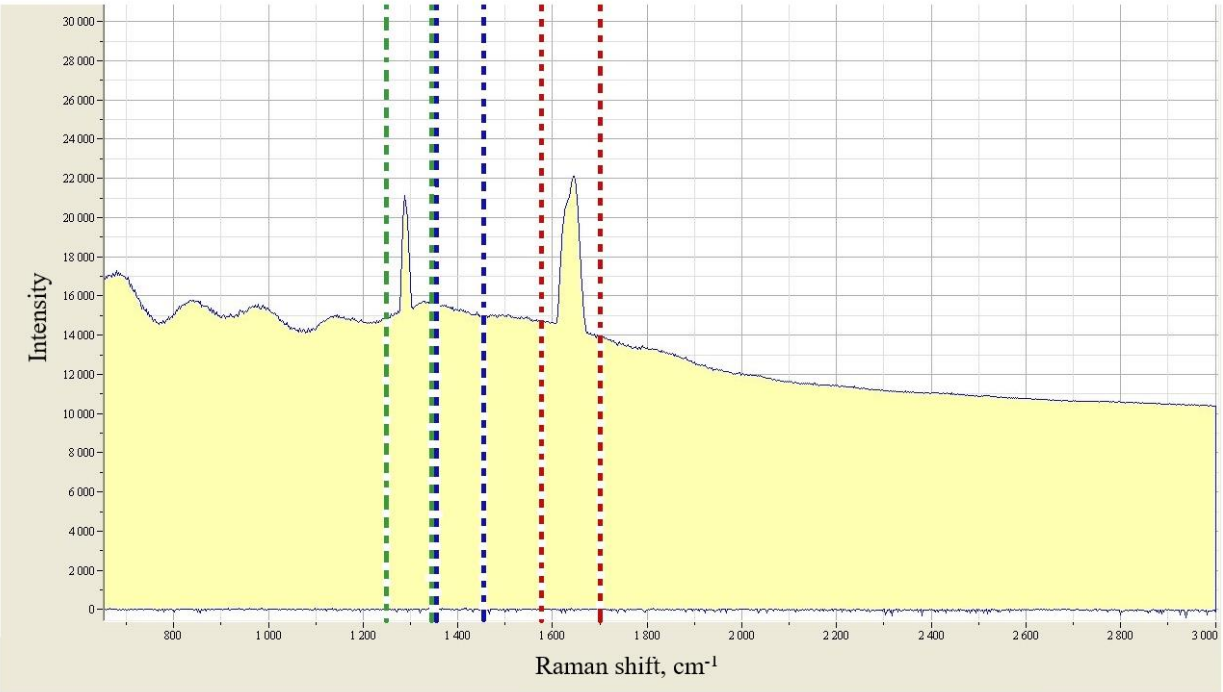

Fig. 40. Total averaged Raman spectrum of the filter surface with selected wavenumber ranges. The spectrum was obtained with an exciting line of 632.8 nm, H=500 μm, and S=100 μm.

Thereafter the spectral map of the surface is determined in these regions of wavenumbers by the intensity of the signal (Fig. 41). Moreover, if the Raman signal is observed only in the first selected region of the spectrum at some point, then the pixel color will be green, if in the second it will be red. If there is an intense signal in both selected regions in the spectrum, then this pixel will be indicated as yellow. As already noted, the signal intensity is determined by the color saturation.

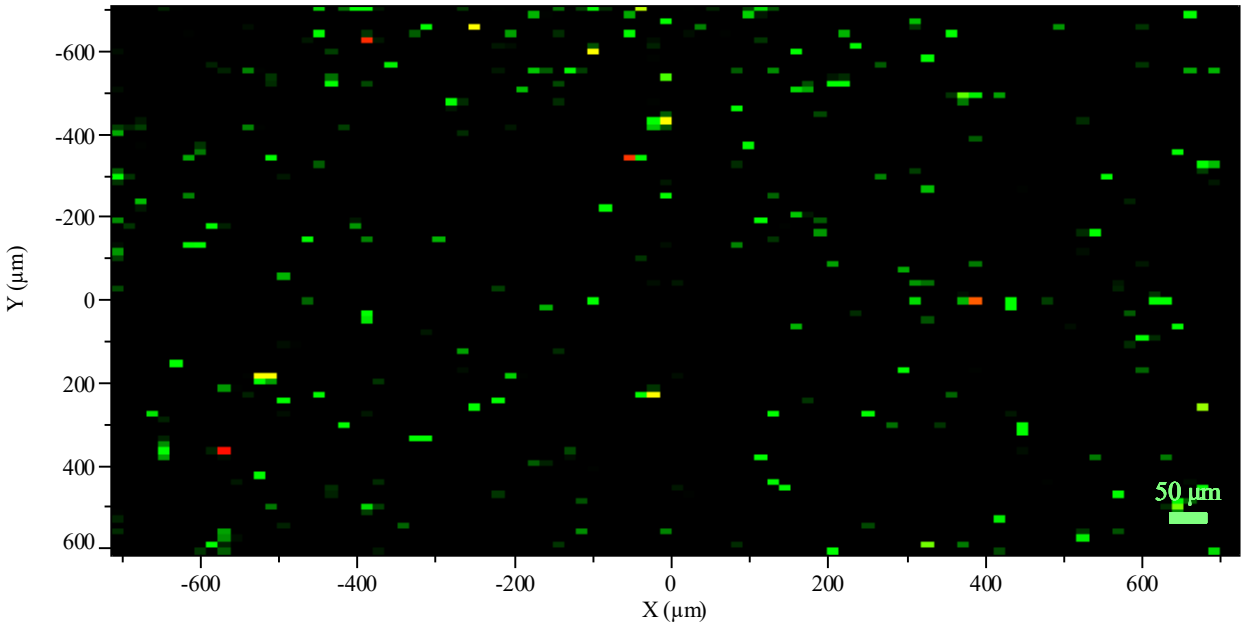

Fig. 41. Raman Spectral map of the surface of a contaminated filter with respect to two limited ranges of wave numbers: 1250-1350 cm^{-1}, indicated as green pixels, and 1575-1700 cm^{-1}, indicated as red pixels.

The Raman spectrum referring to the yellow pixels is characterized by intense peaks at 1293 cm^{-1} and 1646 cm^{-1} (Fig. 42) and corresponds to 2,3-difluorocinnamic acid. It should be noted that the spectrum shows a general fluorescent background, which manifests itself in a moderate increase in background intensity.

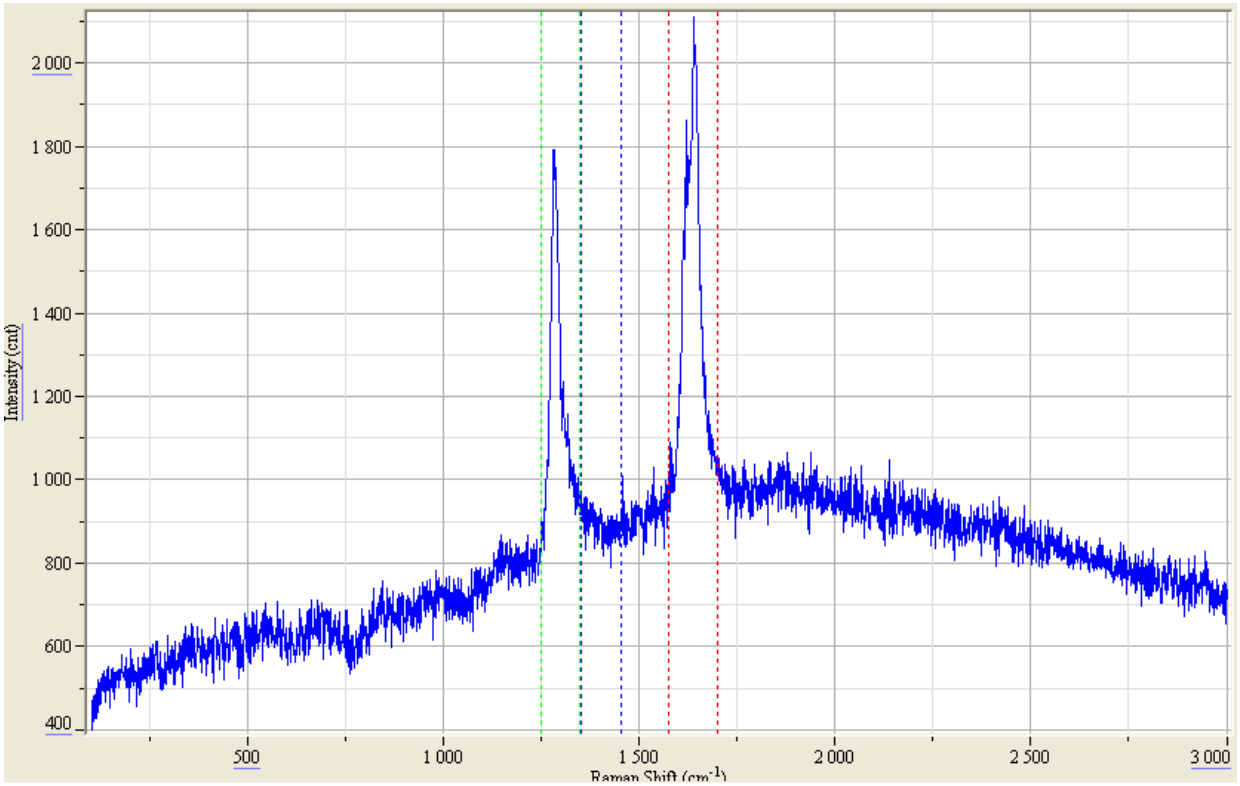

Fig. 42. Raman spectra of 2,3-difluorocinnamic acid ($C_9H_6F_2O_2$). The spectrum was obtained with an exciting line of 632.8 nm, H=500 μm and S=100 μm.

Spectral analysis allows one to align the fluorescent background, while the spectrum takes the usual form (Fig. 43).

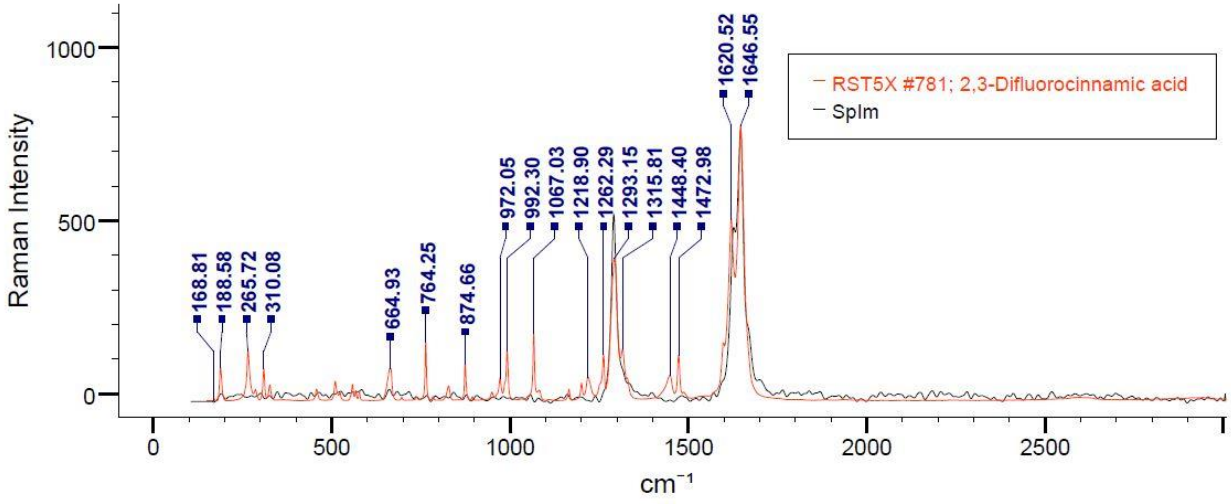

Fig. 43. Raman spectra of 2,3-difluorocinnamic acid ($C_9H_6F_2O_2$). The spectrum was obtained with an exciting line of 632.8 nm, H=500 μm and S=100 μm.

2,3-difluorocinnamic acid is quite common on the surface of the investigated filter. This is confirmed by the distribution of the corresponding yellow pixels on the spectral map of the surface and the presence of distinct characteristic peaks in the total spectrum.

Unfortunately, it is not always easily possible to find and identify the components of a substance. A manual spectrum search revealed another frequently occurring compound, the signal intensity of which was not sufficient to make a visually visible contribution to the overall spectrum. This region is bounded by blue in Fig. 40 and corresponds to the range of wavenumbers 1350-1450 cm^{-1}. The spectral map defined by this range is shown in Fig. 44.

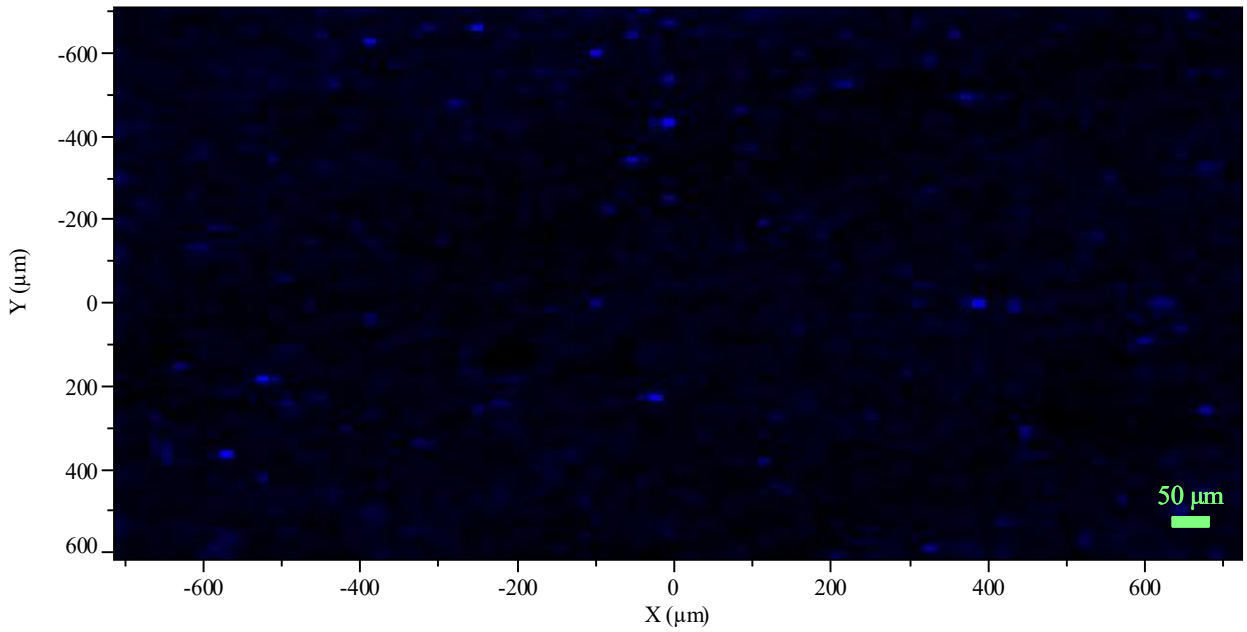

Fig. 44. Raman spectral map of a contaminated filter surface relative to the wavenumber range 1350-1450 cm^{-1}, indicated as blue pixels.

This compound is also distributed over the entire surface of the studied area. The spectrum of the most intense signal of this substance is characterized by two closely spaced peaks (Fig. 45).

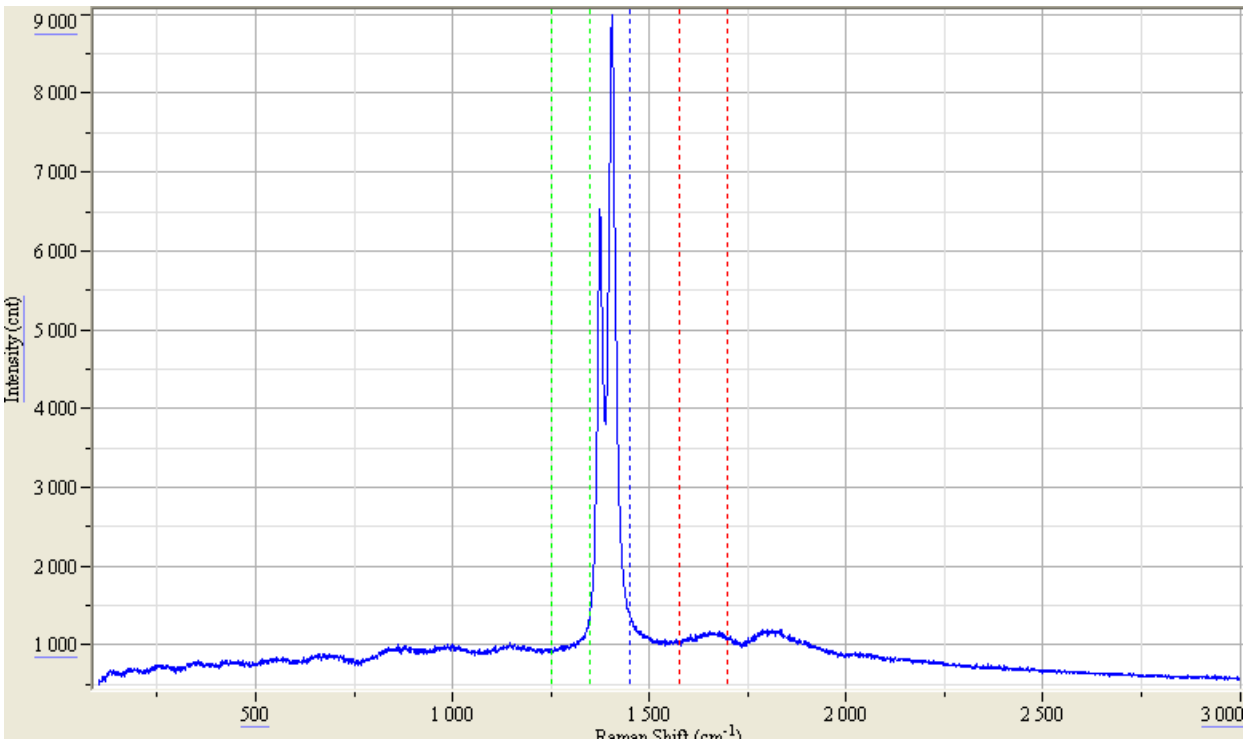

Fig. 45. Raman spectrum of acriflavine hydrochloride ($C_{27}H_{27}Cl_3N_6$). The spectrum was obtained with an exciting line of 632.8 nm, H=500 µm, and S=100 µm.

The spectral analysis identified the component as acriflavine hydrochloride (Fig. 46), whose characteristic property is a red-brown color that is visually distinguishable on the filter surface.

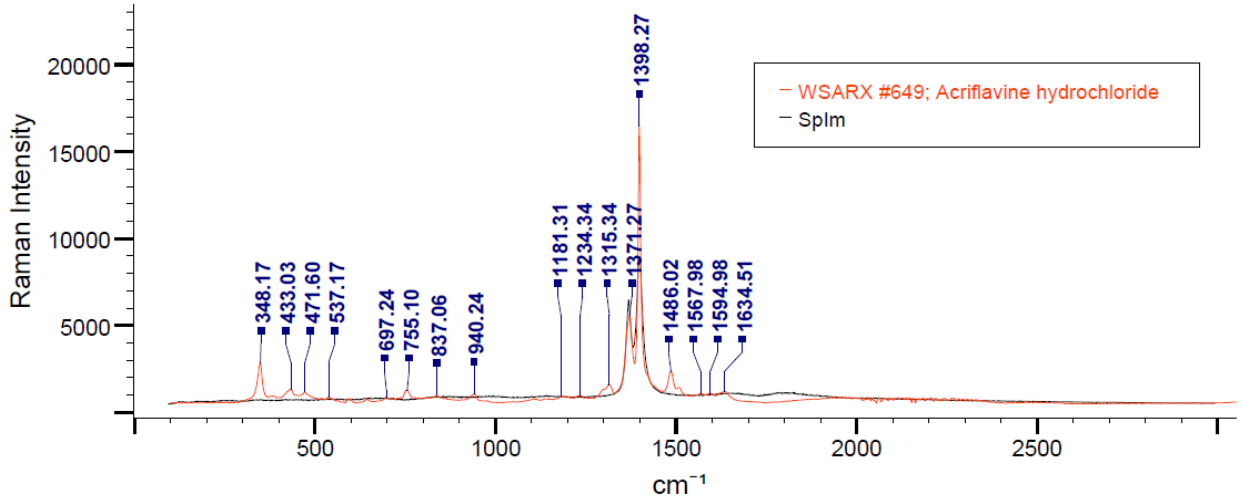

Fig. 46. Raman spectrum of acriflavine hydrochloride ($C_{27}H_{27}Cl_3N_6$). The spectrum was obtained with an exciting line of 632.8 nm, H=500 µm, and S=100 µm.

Both compounds, $C_9H_6F_2O_2$ and $C_{27}H_{27}Cl_3N_6$, were determined with a probability of 90-92%. This is a good indicator when studying multicomponent materials, among which there are

fluorescent components. In addition to the prevailing 2,3-difluorocinnamic acid and acriflavine hydrochloride, other compounds were found on the filter surface. Of particular note are those whose analysis showed a 95-99% chance of coincidence. There were two such components, titanium oxide and phenakite (Fig. 47). Their presence in the examined area is small, which makes it impractical to compile spectral maps of their distribution.

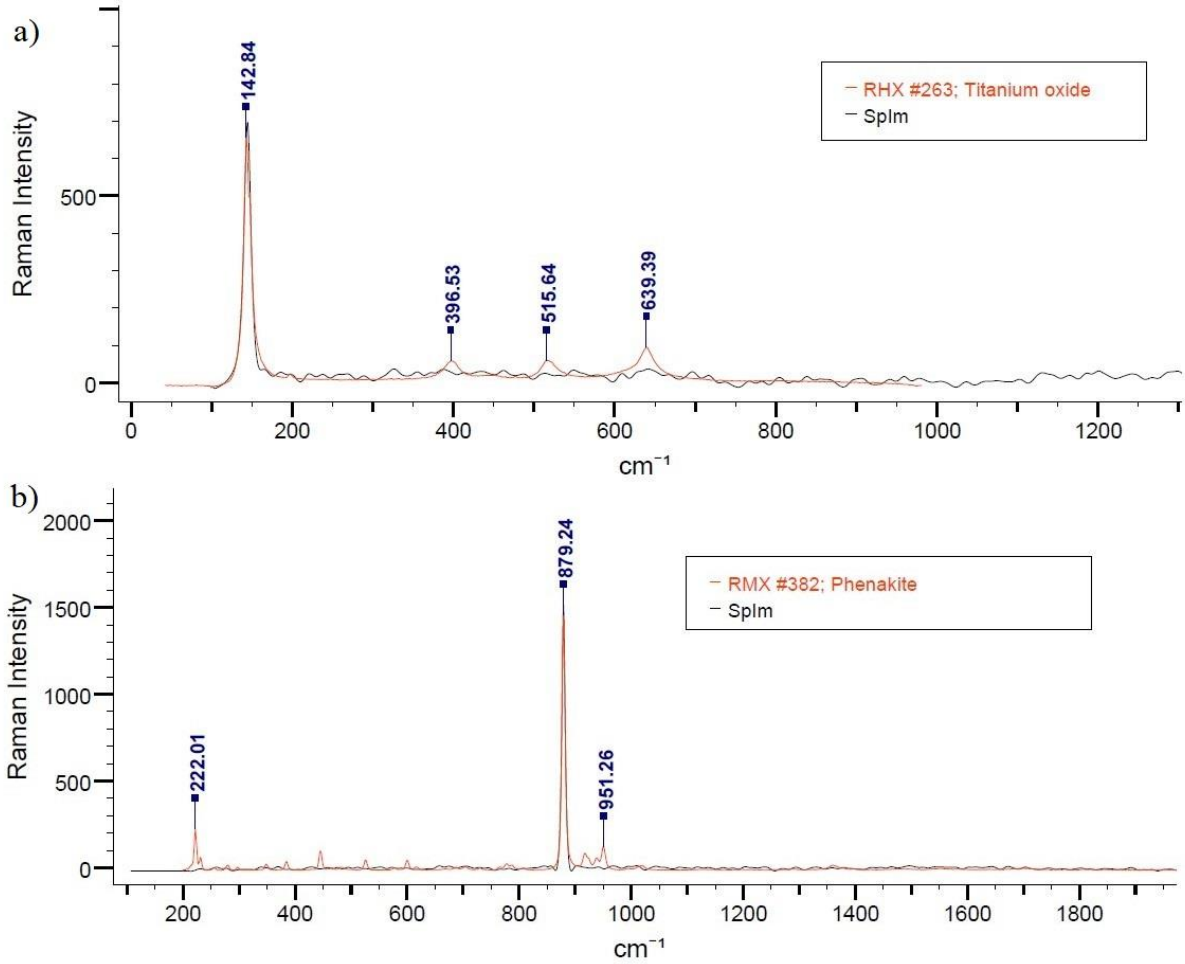

Fig. 47. Raman spectrum of a) titanium oxide (TiO_2); b) phenakite (Be_2SiO_4). Spectrums were obtained with an exciting line of 632.8 nm, H=500 μm, and S=100 μm.

Noticeable that in contrast to the widespread titanium oxide, phenakite is a fairly rare mineral, used mainly as collection material.

3.4.1. Results

In conclusion, one can say that no traces of plastic and its derivatives were found within the studied filter region. However, this result is not absolute, and it is impossible to conclude that there is no plastic in the studied aqueous medium based on this result. This is primarily due to the small

area analyzed. The area of the entire filter is about 2 cm^2, while the spectral map was compiled for a region of about 1 mm^2. Obtaining spectra over the entire surface would be time consuming.

Secondly, even if the entire surface of the filter would be completely and detailed examined, one cannot say for sure that it contains samples of all the compounds present in the contaminated aqueous medium.

And finally, one should remember that the larger the area under study, and the higher the resolution of the spectral map one want to get, the more difficult the analysis of the resulting data. In this case, it becomes practically impossible to process all the obtained Raman spectra, which ultimately means the impossibility of detecting all substances present on the surface.

SUMMARY

The phenomenon of Raman scattering of light was discovered more than 90 years ago and has since been widely used in physics, chemistry, and many other fields. The Raman spectroscopy method has significant advantages over other analytical methods. Among the main advantages, it is non-contact, absence of requirements for sample preparation, and lack of destructive effect on the sample. The main disadvantages of the method that limit its application are due to the presence of strong background radiation as a result of fluorescence of some samples, as well as low signal intensity at a low material activity.

The main practical task of this work was to find certain substances (traces of microplastics) on the filter surface. To solve this problem, a spectral map of a limited area was compiled. Analysis of the obtained data allows one to conclude that the substances in question are not present in the studied filter area, but it does not provide any information about the rest of the surface. The experiment showed the impossibility to make a detailed map of the entire filter surface due to the large time costs, as well as difficulties in subsequent analysis. Second significant drawback was the strong fluorescence detected when working with the filter, and not allowing to get all the information about the chemical composition of the studied area. Thus, the use of the mapping function by the Raman spectrometer is limited in the case of relatively large materials and highly fluorescent substances. However, the Raman spectroscopy method has proved to be very accurate and practical to obtain a single spectrum of non-fluorescent samples.

REFERENCES

[1] Svanberg, Sune. *Atomic and molecular spectroscopy: basic aspects and practical applications*. Vol. 6. Springer Science & Business Media, 2012.

[2] Schrader, B. "Infrared and Raman spectroscopy: Methods and applications VCH Publishers." *Inc., New York, USA* (1995).

[3] Schrötter, H. W., and H. W. Klöckner. "Raman scattering cross sections in gases and liquids." *Raman spectroscopy of gases and liquids*. Springer, Berlin, Heidelberg, 1979. 123-166.

[4] Smith, Ewen, and Geoffrey Dent. *Modern Raman spectroscopy: a practical approach*. John Wiley & Sons, 2019.

[5] Ismail, Kaaya. *Fabrication and characterisation of SERS substrates through photo-deposition of Gold Nanoparticles.* PhD thesis, The Abdus Salam International Center for Theoretical Physics, Italy, 2015.

[6] Graves, P. R. G. D. J., and D. Gardiner. "Practical raman spectroscopy." *Springer* (1989).

[7] Li, Zhiyun, et al. "Raman spectroscopy for in-line water quality monitoring—Instrumentation and potential." *Sensors* 14.9 (2014): 17275-17303.

[8] Bakeev, Katherine A., ed. *Process analytical technology: spectroscopic tools and implementation strategies for the chemical and pharmaceutical industries*. John Wiley & Sons, 2010.

[9] Vandenabeele, Peter. *Practical Raman spectroscopy: an introduction*. John Wiley & Sons, 2013.

[10] Nasdala, L. U. T. Z., et al. "Raman spectroscopy: analytical perspectives in mineralogical research." *Spectroscopic methods in mineralogy* 6 (2004): 281-343.

[11] Li, Da-Wei, et al. "Recent progress in surface enhanced Raman spectroscopy for the detection of environmental pollutants." *Microchimica Acta* 181.1-2 (2014): 23-43.

[12] Colthup, Norman. *Introduction to infrared and Raman spectroscopy*. Elsevier, 2012

[13] Vityaz, Peter, Nikolai Svidunovich, and Dmitry Kuis. Nanomaterial science. Litres, 2017 (in Russian).

[14] Shamina, L.A., et al. "Analysis of the correlation of the spectral characteristics of Raman scattering and autofluorescence of human skin in the visible and near infrared ranges." Information technology and nanotechnology. 2018 (in Russian).

[15] McCreery, Richard L. *Raman spectroscopy for chemical analysis*. Vol. 225. John Wiley & Sons, 2005.

[16] Long, Derek Albert. "The Raman effect: a unified treatment of the theory of Raman scattering by molecules." (2002): 541-564.

[17] Kang, Yilan, et al. "An application of Raman spectroscopy on the measurement of residual stress in porous silicon." *Optics and lasers in engineering* 43.8 (2005): 847-855.

[18] Kopitsyn, D.S., et al. "The choice of substrate material in experiments on giant Raman spectroscopy." Bashkir Chemical Journal 21.4 (2014) (in Russian).

[19] Strommen, Dennis P., and Kazuo Nakamoto. "Resonance raman spectroscopy." *Journal of Chemical Education* 54.8 (1977): 474.

[20] Drago, Russell S. *Physical methods in chemistry*. No. 540 D7. 1977.

[21] Petrov, Dmitri V. "Raman spectroscopy of optically trapped particles." *Journal of Optics A: Pure and Applied Optics* 9.8 (2007): S139.

[22] Fayer, Michael D. *Ultrafast infrared and Raman spectroscopy*. Vol. 26. CRC Press, 2001.

[23] https://wikipedia.org/wiki/Coherent_anti-Stokes_Raman_spectroscopy/

[24] Evans, Conor L., and X. Sunney Xie. "Coherent anti-Stokes Raman scattering microscopy: chemical imaging for biology and medicine." *Annu. Rev. Anal. Chem.* 1 (2008): 883-909.

[25] Kudelski, Andrzej. "Analytical applications of Raman spectroscopy." *Talanta* 76.1 (2008): 1-8.

[26] Sharma, Bhavya, et al. "SERS: Materials, applications, and the future." *Materials today* 15.1-2 (2012): 16-25.

[27] Nakamoto, Kazuo. "Infrared and Raman Spectra of Inorganic and Coordination Compounds." *Handbook of Vibrational Spectroscopy* (2006).

[28] Kneipp, Janina, et al. "Novel optical nanosensors for probing and imaging live cells." *Nanomedicine: Nanotechnology, Biology and Medicine* 6.2 (2010): 214-226.

[29] Isemann, Andreas. "Laser requirements and advances for Raman techniques." (2013).

[30] https://wikipedia.org/wiki/Helium-neon_laser/

[31] https://czl.ru/tgroups/the-principle-of-the-spectrometer/

[32] Kang, Yilan, et al. "An application of Raman spectroscopy on the measurement of residual stress in porous silicon." *Optics and lasers in engineering* 43.8 (2005): 847-855.

[33] Griffiths, Peter R., and James A. De Haseth. *Fourier transform infrared spectrometry*. Vol. 171. John Wiley & Sons, 2007.

[34] Rodrigues, Lillian, Yuri Winche, and Gary B. Hughes. "Spectrometer subsystem for a CubeSat mission to test remote laser-evaporative molecular absorption (R-LEMA) spectroscopy concept in the space environment." *CubeSats and NanoSats for Remote Sensing II*. Vol. 10769. International Society for Optics and Photonics, 2018.

[35] Ellis, Gary, et al. "Routine analytical Fourier transform Raman spectroscopy." *Analyst* 114.9 (1989): 1061-1066.

[36] Keller, Stefan, et al. "Application of near-infrared-Fourier transform Raman spectroscopy in medical research." *Journal of Raman Spectroscopy* 25.7-8 (1994): 663-671.

[37] Xue, Gi. "Fourier transform Raman spectroscopy and its application for the analysis of polymeric materials." *Progress in polymer science* 22.2 (1997): 313-406.

[38] https://horiba.com/

[39] Widenhorn, Ralf, et al. "Temperature dependence of dark current in a CCD." *Sensors and Camera Systems for Scientific, Industrial, and Digital Photography Applications III*. Vol. 4669. International Society for Optics and Photonics, 2002.

[40] Lazovsky, L. "Charge-coupled devices: a precise view of the world." AVTEX. St. Petersburg. 6 (2005) (in Russian).

[41] Schmid, Thomas, and Petra Dariz. "Raman Microspectroscopic Imaging of Binder Remnants in Historical Mortars Reveals Processing Conditions." *Heritage* 2.2 (2019): 1662-1683.

[42] Karlen, Sylvain, et al. "Quantitative micro-Raman spectroscopy for partial pressure measurement in small volumes." *Applied spectroscopy* 71.12 (2017): 2707-2713.

[43] Horiba Jobin Yvon. Training "LabRAM Spectrometer and LabSPEC Software"